TÉCNICO LISBOA

Optimizing Energy Consumption in a Municipal Building

Miguel Alexandre Correia Gameiro

Thesis to obtain the Master of Science Degree in

Electrical and Computer Engineering

Supervisor(s): Prof. João Filipe Pereira Fernandes
Prof. Paulo José da Costa Branco

Examination Committee

Chairperson: Prof. João Fernando Cardoso Silva Sequeira
Supervisor: Prof. Paulo José da Costa Branco
Member of the Committee: Prof. Susana Margarida da Silva Vieira

November 2018

Declaration

I declare that this document is an original work of my own authorship and that it fulfills all the requirements of the Code of Conduct and Good Practices of the Universidade de Lisboa

Acknowledgments

This dissertation marks the final of one more cycle in my life. It started in September of 2012 when I started the course on Electrical and Computer Engineering in Instituto Superior Técnico. I can classify it as the most intense learning cycle of my life.

I started my master in September of 2015. That semester, I was mostly finishing my graduation. My only master course was Electrical Machines with Professor Paulo Branco. Since then, I have been working there. During these time, I have known many generations of people which worked there. All of them had a notorious group spirit. For all these people I want to thank and acknowledge on all the companionship I had these years. In particular, I want to thank Professor Paulo Branco on guidance of this team during these years and, in particular, my dissertation in these last months.

I want to thank to all my friends in a special way, for their friendship. In particular, to Francisco Silva, Hugo Loureiro and Paul Schydlo for their support in last moments of this dissertation.

I want to thank my family for all support given during one more cycle of my life, in particular, this dissertation.

I want to give a thank you note to *meteoblue* website for giving me a free access to meteorological history data on Cascais city during the course of this dissertation.

Resumo

Os sistemas AVAC (Aquecimento, Ventilação e Ar Condicionado) são sistemas críticos na sociedade moderna. A crescente necessidade aquecimento ou arrefecimento têm aumentado o numero de AVACs necessários. Estudos indicam que estes estão entre os sistemas estão entre os sistemas que mais energia consomem mundialmente. Um AVAC é um investimento a longo prazo, instalado com base num estudo efetuado sobre as necessidades do edifício. No entanto, é possível verificar que muitos destes sistemas presentes em edificios comerciais consomem energia em excesso.

Uma solução comum na literatura é usar controlo predictivo. No entanto é frequente que estas soluções sejam económicamente inviáveis. Aqui, é a apresentada uma estratégia de otimização baseada em controlo ótimo. O controlo é efectuado com base na num conjunto de modelos de predição, que permitem avaliar o desempenho do AVAC em função do cenário de funcionamento.

Esta dissertação apresenta um caso de estudo no Cascais Center, onde é aplicada a estratégia de controlo ótimo, com o objetivo de melhorar o custo energético e o conforto térmico. Neste caso, é encontrada uma melhor temperatura de comando para o chiller, recorrendo meta-heuristicas NSGA-III e PSO. A predição é efetuada com base em aprendizagem automática, utilizando NARX Neural Network e Takagi-Sugeno, recorrendo a PCA para extração de informação. Os resultados obtidos indicam a necessidade de trabalho futuro no sentido de melhorar a aquisição de dados, robustez de predição e a estimativa de conforto térmico.

Palavras-chave: AVAC, otimização, controlo ótimo, meta-heuristicas, modelos orientados a dados, PCA

Abstract

HVAC (Heating, Ventilation and Air Conditioning) systems are critical in modern human activity. The increasing demand for heating and cooling applications increases the number of HVACs. Based on many studies, these are some of the most energy consumer systems worldwide. An HVAC is, usually, a long term investment. It is installed having in account specific necessities of the building. However, one can find that often HVAC from commercial consume energy in excess.

A common solution found on literature is to use model predictive control. However, these solutions maybe not be viable economically. Here, it is presented an optimal control framework for the optimization of HVACs. This framework uses data-driven models to predict the system dynamics in the chosen scenario.

This dissertation shows a start to end case study on Cascais Center, where it is applied an optimal control framework, aiming to improve energy costs and thermal comfort. In this case, the optimized variable is the chiller temperature setpoint, using NSGA-III and PSO meta-heuristics. The models are base on data-driven predictors, the NARX Neural Network and Takagi-Sugeno, with improved feature extraction achieved by using PCA. Hence, it is presented a methodology for variable selection and feature extraction. The predictors performance is improved based on data analysis considerations. The results a need for further work on data acquisition, prediction robustness and thermal comfort estimation.

Keywords: HVAC, optimization, optimal control, meta-heuristics, data-driven models, PCA

Contents

List of Tables

List of Figures

Chapter 1

Introduction

1.1 Motivation

HVAC (Heating, Ventilation and Air Conditioning) systems are critical in modern human activity. Society has becoming more dependent on temperature control applications for reasons like: food refrigeration, computerization and networking, more complex industry and manufacturing processes. In all these cases, the need for these systems is increasing and becoming more important in energy consumption pattern around the world. This reason makes HVAC systems one of the most interesting to optimize.

The worldwide electrical energy demand increases early, requiring more and more electrical energy production. In part because of the appearing of new and more powerful applications but also because of its preference over other energy forms. There is a common known world's effort in reducing electrical energy demand, implying a need of optimizing the actual usage. The evolution of world electrical energy consumption is presented in Figure 1.1.

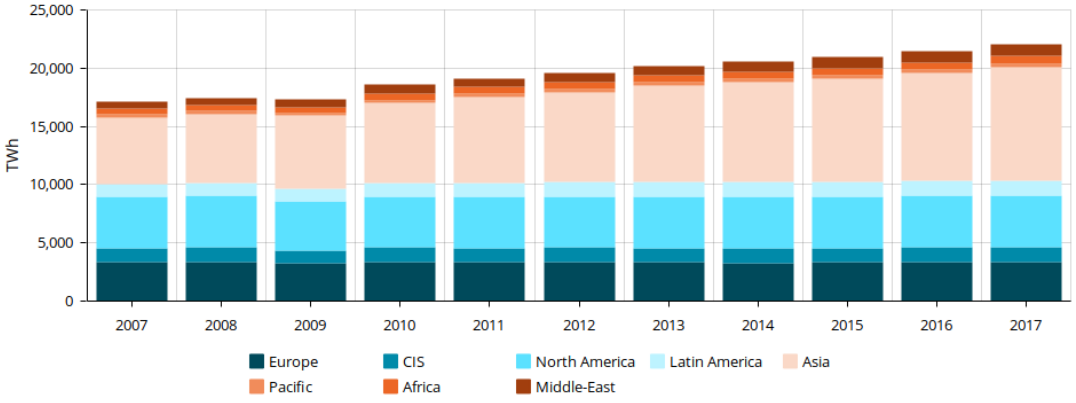

Figure 1.1: World electrical energy consumption [1]

This graph shows an increasing of more than 25% in electrical energy consumption worldwide in last 10 years. In part, this is due to a growing dependence on HVAC systems. These are very common in industry, where temperature can be crucial, and commercial and office buildings, in order to maintain thermal comfort and air quality inside and over the years started to be more common in residential

buildings also. Australia's electrical energy regulatory and the University of Michigan estimated the typical energy consumption pattern in office buildings of Australia and residential buildings of United States of America shown in Figure 1.2.

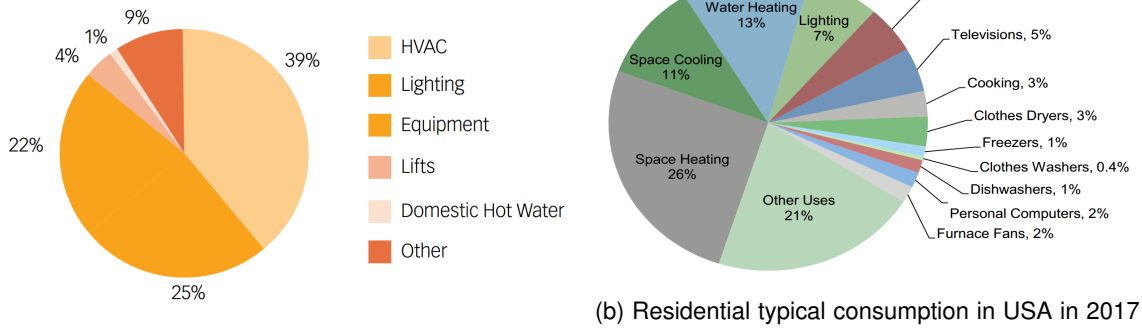

(a) Office buildings typical consumption in Australia [2]

(b) Residential typical consumption in USA in 2017 [3]

Figure 1.2: Electrical energy consumption patterns

In both cases the energy spending in for both heating and cooling are the highest energy consumption application (both in a range of 35% to 40%), having an high impact in energy bill. This consumption can't be isolated, the increasing usage of another devices can influence the thermal load, for example, in an office building computers are extra thermal loads for the cooling system since they produce heat.

In commercial buildings, HVAC systems are very important in keeping the thermal comfort and the air quality inside. Its main functions are to control temperature, humidity, air renewal, filtration of airborne particles and air movement inside. All these factors influence people's perception in a non-linear way, having opposite effects for different people.

In a consumption optimization perspective it is useful to have a centralized model in charge of controlling the operation parameters. This allows making use of the most important principal in a system optimization strategy: consume just the minimum amount, not an amount needed for a general case of the same type. This is the reason for using a data dependent approach for optimizing the system usage.

1.2 Objectives

The objective of this dissertation is to study a methodology to improve an HVAC efficiency based on a non-intrusive external system. For an HVAC, improving efficiency in an optimization point of view is to minimize the energy cost and maximize the thermal comfort.

An HVAC often serves a building for a long time, being a long term investment. During this time, the necessities may change and the technology advances. In commercial buildings, it is common to find HVACs consuming much more energy than it is needed and the total or partial substitution is not economically viable. In this sense, the idea is to create an external, non intrusive system, which can provide support to the user in improving the HVAC utilization. The system bases its decision on information about meteorological variables and human occupancy, to adapt the HVAC to the real necessities.

In this dissertation, it is presented a case study made in Cascais Center, a municipal building which

includes an offices area and a commercial area. The goal is to optimize the chiller setpoint using meta-heuristic based optimization with data-driven models. The case study made is focused on two commercial stores, Loja do Cidadão and Social Security store, which represent the fastest occupancy dynamic and the highest concentration of people there. In Cascais Center the system can indicate the optimized setpoint, based on predictions made, considering a reasonable time window for people to change it. This case study also serves as a way to analyze the methodology made here, and check its scalability to other HVAC systems optimizations based on energy cost and thermal comfort.

1.3 Previous Work

There are many examples of developed work in optimizing HVAC systems, where many approaches were followed. The challenges are many, starting in the definition of the optimization method and scenario, the modeling of the HVAC system and even on the thermal comfort estimation.

On [4], it is developed a case study on a building from Instituto Superior Técnico, where the main focus is to optimize the chiller setpoint from the HVAC system. The observers used two different models, the grey-box model and the NARX Neural Network. A similar study was developed on [5]. In this work, it was developed a simplified thermal model, to be used with the ASRHRAE-55 thermal comfort model. The optimization was based on genetic algorithms. A master thesis [6] from the university of Iowa developed a study optimization of HVAC systems using data-driven modeling. Many different observers where tested and compared from different metrics point of view. The optimization is based on evolutionary algorithms.

More recent studies focus on using energy price to lower energy consumption costs by using the price variation information. In [7], it used the an optimal control strategy to use the energy price schedule. The thermal comfort was given by the occupants in the room in real time, using an application on their cell-phones. In [8], also uses the energy price to lower the costs, but the main focus, is in the modeling part, in particular, the input variable selection for the observers. The occupancy is predicted based on previous data, related to the week day, the time during day and the weather season.

Many studies focused in the development of the prediction models. In [9], there are advantages, showed in predicting the temperature in a relative way, by predicting the sample differences. If applied, the complexity of the model for prediction can be lower. In [10], in 2013, applied model predictive control to the HVAC system, using neural network to predict the interior temperature and the consequent thermal comfort. In parallel, sensors were used to correct predicted values. In [11], showed that there can be advantages in using observers with many outputs when predicting interior temperatures in adjacent rooms. This way, the mutual influences in predicted temperature dynamics can be modeled by the observer.

In [12], from the University of Algarve and IDMEC from IST, in 2012, used Artificial Neural Networks (ANN) to predict the Predicted Mean Vote (PMV). While it can improve the accuracy by adapting to the case study, it also can speed-up its calculation. The value of PMV as it is described on ASRHAE-55 is calculated by an iterative method [13].

1.4 Thesis Outline

This dissertation is divided in 7 different chapters (including this one) and two appendixes. During these, it is described the end to end method applied during Cascais Center case study. This includes the main principles and concepts followed and description of the application on the case study considered.

- **Chapter 2**: there is a brief overview on Cascais Center building a its main characteristics. The building is presented with blueprints for considered floors and with a description on the selected thermal zones and the main characteristics of the HVAC system. This relates with the data acquirement periods and constraints. Some preliminary results are presented in order to give a first impression on the data in a statistical point of view.
- **Chapter 3**: there is a presentation on the main principles followed in optimization. This includes a presentation on the used cost function construction, meta-heuristic methods and the multi-optimization dealing based on Pareto optimal. For both objectives, it is presented the mathematical description and simplification considerations associated. There is a presentation on used algorithms and on Pareto optimization method.
- **Chapter 4**: there is a description on main principles followed on the observers and their implementation results. It starts with the pre-processing, done on the acquired data and information extraction on sensor-less acquired data. On the observer construction principles, there is a description on the used prediction models, the selection on input variables and how their usage can improve the supervised learning performance. Then, an implementation overview with the main results obtained.
- **Chapter 5**: there is a description on how the observers are integrated into an optimization method as a physical model. Then, the method of selecting the optimal point based on the optimization results, considering the case study. An important issue is to define the usage scenarios and how it is applicable to the Cascais Center case study, based on this construction and on specifics on Cascais Center.
- **Chapter 6**: the main results obtained on Cascais Center case study are presented along with first impression conclusions. The main incongruousness parts on the results pointed and described.
- **Chapter 7**: the main conclusions about the method and results obtained during dissertation are presented. Along with that, there are the future logical steps which can be followed to continue and improve the work done.

Chapter 2

Cascais Center Presentation

2.1 Building

The Cascais Center is a building situated in Cascais city. The building has 7 floors, several public service stores and some offices, which belong to the city. This topology of building concentrates a big amount of people, some working there, some using the services provided. A photo of Cascais Center building is shown in Figure 2.1.

Figure 2.1: Cascais Center photo [14]

At bottom floors there are many common areas. There are 3 stores: Loja do Cidadão, National Insurance and CTT (Correios de Portugal, SA), a cantine, a computer team open-space and wide space halls and corridors. In these floors, there is more people and movement getting in and out of the building. These spaces are used by workers and also clients for these stores. At top floors there are office cabinets for non-public attendance workers. There are less density of people, separated by different divisions.

2.2 Thermal Zones

The building has an heterogeneous density of people inside and on space distribution. This fact implies, also, an heterogeneous influence on HVAC system dynamics. For instance, an open space store like Loja do Cidadão has a different influence on the HVAC dynamics than the office cabinets. During dissertation, the focus was on two commercial spaces: Loja do Cidadão and the Social Security store.

Before going further, there are two important concepts to define first based on [15] reference definitions: thermal zone and thermal space. A thermal zone is a part of the building controlled a single sensor. A thermal space is a part of the building, not necessarily separated by walls and floors. A thermal space may have several thermal zones, but a thermal zone could be a part of a thermal space.

Applying these concepts to the Cascais Center case, the interest is to make the thermal zones of the new system roughly coincide with the thermal spaces identified empirically inside the chosen stores. In other words, the National Insurance store is one thermal zone and Loja do Cidadão can be divided in two thermal zones considering this dissertation project. The National Insurance store shares the air handler with many other building divisions, but Loja do Cidadão has its own air handler. The temperature inside National Insurance store is almost homogeneous. Contrarily, at Loja do Cidadão one has the thermal space divided in two thermal zones, each on with its temperature sensor to acquire the temperature evolution (see chapter 2.4).

Loja do Cidadão and National Insurance store are relatively different when it comes to occupancy dynamics. The type and amount of services on both are different. This may imply different habits on clients, on time schedules in which the service is used, speed of attendance and many other factors. The office hours are also different on both stores, as it is presented on Table 2.1.

Table 2.1: Office hours from Loja do Cidadão and Social Security stores in Cascais Center

Store	Week Day	Office Hours
Loja do Cidadão	Monday - Friday	09h00m - 18h00m
Social Security	Monday - Friday	09h00m - 16h00m

The blueprints of floor 0 and floor 1 are shown in Figure 2.2 and Figure 2.3, respectively, with the stores marked with dark grey background.

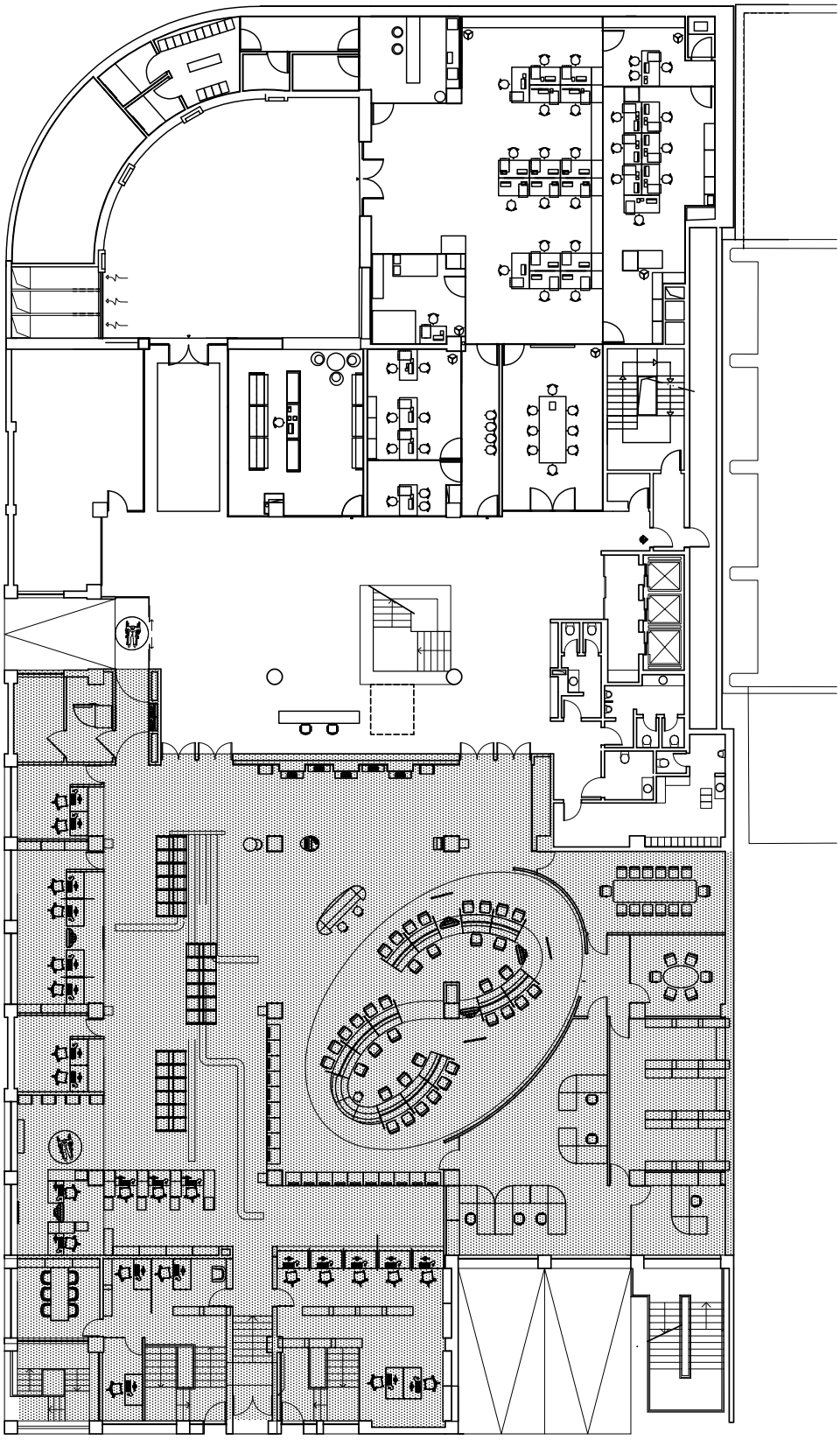

Figure 2.2: Floor 0 from Cascais Center blueprint

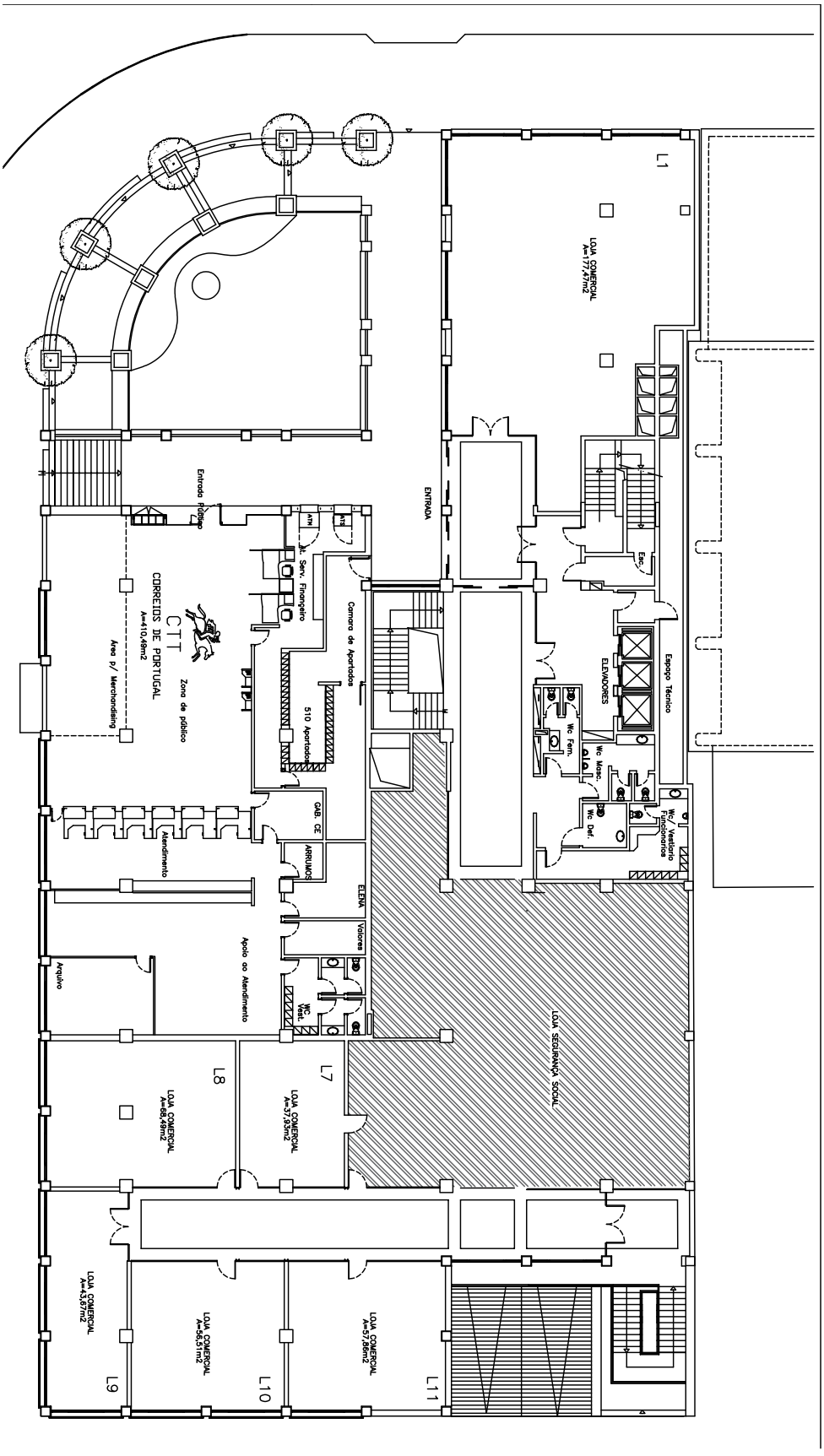

Figure 2.3: Floor 1 from Cascais Center blueprint

Portugal is a tradicionally hot country and Cascais is one particlar case of it. The annual average

temperature in Cascais is roughly 16^{o}C and an high percentage of sunny days. The number of hours with sun in Portugal is 2799 hours per year. Both stores have big windows spread by the their walls being highly affected by the solar radiation entering.

2.3 HVAC System Caracterization

HVAC systems follow the same base components but are often customized to the specific necessities of the client. When installing a new one, there is usually a specific project. The components chosen strongly depends on building's characteristics. As an example, all water ducts have to be chosen based on building.

The HVAC system installed at the Cascais Center have 3 main parts: chillers and pumps, which makes the heating and/or the cooling water, the air handlers, which heat/cool the air, and also the the air renewal and improve air quality, and the fans, which control the air flux inside. The chillers and pumps part are common for all building thermal zones. They define the operation mode for the system (heating or cooling). For the air renewal and circulation, there are two different subsystems: one for the common spaces and another for the office cabinets spaces. In Figure 2.4, it is presented a simplified diagram of the Cascais Center's HVAC system, and its main components only.

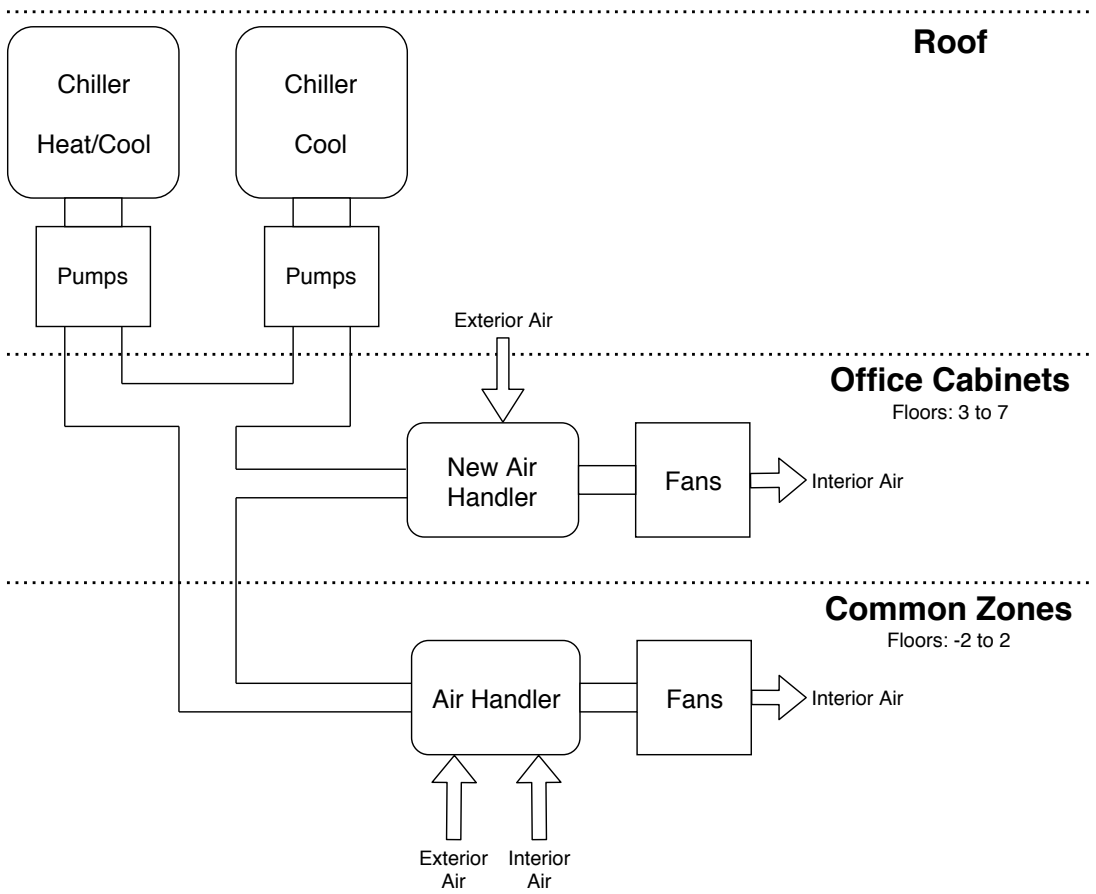

Figure 2.4: Diagram of HVAC from Cascais Center

The HVAC system has two operation modes: heating and cooling. The difference (besides some

configuration) is having one or two chillers and their associated pumps turned ON. In Portugal, there is usually a higher need for cooling than for heating. In Cascais Center HVAC, the heating power is 219.5 kW and the cooling power is 380.4 kW. The main components of Cascais Center HVAC are presented in Table 2.2.

Table 2.2: Nominal power of main HVAC modules

Module	Nominal Power Heating	Nominal Power Cooling
Heat/Cool Chiller	219.7 kW	231.0 kW
Cool Chiller	-	150.0 kW
Air Handler	13.2 kW	17.0 kW
New Air Handler	09.9 kW	44.8 kW
Fans	54.0 W/97.0 W/111 W	

For all these modules, there are commands defining the operating point, making it spend more or less electrical energy. For each of the chillers, there is a setpoint, that controls the water temperature. For the air handlers and new air handlers, there is also a temperature setpoint which controls how much energy is absorbed by the water circulating. For the air handlers case, it controls how the mixture of interior and exterior air is done to maintain the air quality inside. The fans are dimensioned to the space volume, having different nominal power values. Their command is air speed input control.

2.4 Data Acquisition

The main objective for these measurements is to provide data to data-oriented modeling. When describing the cost function for optimization (see it on Section 3.1), there where two dimensions for the cost: one related to electrical energy consumed and another related to thermal comfort. The loggers used for acquiring data are on Figure 2.5.

(a) Electrical power logger [16] (b) Temperature logger [17]

Figure 2.5: Loggers for acquiring and storing data

On Figure 2.5a it is presented Fluke 1735, used for electric power logging. This device was connected to an HVAC specific switchboard, where all HVAC system devices are connected (except for the air handler of Loja do Cidadão). This way the energy consumption measured are the ones from almost

all system. On Figure 2.5b, it is presented TinyTag Tk-4000, used for interior temperature logging. The acquired temperatures are one on Social Security store and two another on Loja do Cidadão. These are the thermal zones for the system developed by this Thesis, as described on chapter 2.2. The data from the meteorological conditions was gently given by *meteoblue*. On meteorological data, it was stored the evolution of exterior temperature, solar radiation, humidity and wind speed.

The electrical power data and the interior temperature were both acquired with a 5 minutes sampling period. On Fluke 1735, the maximum amount of data stored is about 2 weeks for the current sampling frequency. That is why all measurement periods lasted less than 2 weeks. For meteorological data, the sampling period of acquisition was 1 hour. The method to deal with these different sampling times will be presented later on chapter 4.1.

There were 5 time periods of data acquisition during the course of Thesis development. The main criteria when choosing them was to get data from different weather seasons and different operating modes (heating and cooling). Notice that there were significant constraints on the availability of the material for logging. That is why all of measurement periods occur on class holidays. The acquisition periods are presented in Table 2.3.

Table 2.3: Periods of data acquisition

Reference	First day	Last day	Operating Mode
April 2017	08/04/2017	16/04/2017	Cooling
September 2017	12/09/2017	19/09/2017	Cooling
January 2018	23/01/2018	05/02/2018	Heating
April 2018	27/03/2018	08/04/2018	Heating
June 2018	19/06/2018	02/07/2018	Cooling

These acquirement periods form a dataset with 30 days on heating operating mode and 27 days on cooling operating mode. During the heating period, the chiller setpoint values were 39^{o}C, 41^{o}C and 42^{o}C. On cooling period, the chiller setpoint values tested were 7.5^{o}C, 8.0^{o}C, 8.5^{o}C and 9.5^{o}C.

2.5 The actual electric energy consumption in Cascais Center

Some conclusions about the actual situation in Cascais Center can be taken from the preliminary results obtained with a small amount of pre-processing on top of acquired data. On Table 2.4, some results are presented, from which some conclusions may be taken. Because of the table size, the headers are abbreviated. The average temperatures are presented individually for each store, with the headers SSS (Social Security Store), LCO (Loja do Cidadão - Fan Output) and LCA (loja do Cidadão - Ambiance Temperature). For the thermal comfort case, it is calculated for each store, with SSS meaning Social Security Store and LC meaning Loja do Cidadão.

Table 2.4: Preliminary results on Cascais Center

Acquirement Reference	Energy [kWh]	Energy Cost [€]	Av. Temp. Outside [^{o}C]	Av. Temp. Inside [^{o}C]			Thermal Comfort	
				SSS	LCO	LCA	SSS	LC
April 2017	500	60.10	16.68	21.44	23.15	22.80	1.54	1.60
September 2017	778	91.72	18.54	19.13	22.65	20.88	1.85	1.99
January 2018	620	72.76	11.09	21.68	20.82	20.47	2.17	2.18
April 2018	451	51.85	12.24	22.16	23.84	22.67	2.08	2.08
June 2018	833	98.47	19.53	20.81	23.76	22.94	2.02	2.04

The energy cost on Cascais Center shows an high sensitivity to the outside temperature variation on both operating modes. On cold operating mode, the cost is, on average, higher when compared to the heating operating mode in consequence of an higher energy consumption.

Inside the building, the average temperature stays usually roughly the same as Table 2.4 shows. For the thermal comfort, the situation is a different one. Despite the value is maintained roughly the same, as it is shown on Table 2.4, the results are very different when the situation is analyzed daily. Though the value 2 is a reasonable thermal comfort index, this average value does not characterize the real comfort levels. This is a result of daily values closer to 0 and others closer to 3 (see it in Appendix A). The average is not enough in characterizing the thermal comfort from a statistical point of view.

Chapter 3

Optimization

An optimization bases its principle in finding either a minimum or a maximum for certain set of cost functions, based on the mathematical definition of these costs. By doing this, the objective is to find which criteria which may lead to a better performance on the selected objectives. The optimization in the dissertation project pretends to minimize the energy consumption and maximized provided by the HVAC. refers to the algorithm used to optimize the chiller setpoint based on scenario conditions. The focus is to find the optimal chiller for the environment conditions.

This chapter presents the followed principles to applied to the HVAC optimization Cascais Center case study. That includes the used definition of cost function, for the objectives presented on Section 1.2, the energy cost and thermal comfort definitions, the multi-objective considerations, based on Pareto optimization, and the meta-heuristic algorithms used presentation.

3.1 Cost Function

A cost function is a mathematical way to describe the objectives to achieve. Describing it in a formal mathematical expression allows to use it to find minimum and maximum values on top this. In fact, optimizing the HVAC usage is to minimize the energy consumption while maximizing the thermal comfort. The objective function for these two objectives will give a 2-dimensional value from the inputs selected as a metric of how well accomplished are the objectives. Each of the objectives are represented in one dimension on cost function. The result of cost function is represented in 2-dimensional form as

$$C = \begin{bmatrix} C_E \\ C_T \end{bmatrix} \tag{3.1}$$

where the C_E represents the value of the energy cost objective and the C_T the value of the thermal comfort one. Next, it is explained individually how to calculate the cost on each objective individually.

Electrical Energy Cost

The cost of electrical is divided in two parts: one of them associated with the fixed contract cost and the other with the energy cost. The prices considered during this dissertation are related with the energy cost. In Cascais Center, it is used BTE tariff from the energy provider, with respective prices presented in Table 3.1.

Table 3.1: Energy price tariff on Cascais Center in 2018

Active Energy Price	Year Quarter	Schedule	EUR/KWh
Long Usage	I and IV	Peak Hours	0.1595
		Full Hours	0.1271
		Normal Empty Hours	0.0847
		Super Empty Hours	0.0744
	II and III	Peak Hours	0.1594
		Full Hours	0.1271
		Normal Empty Hours	0.0843
		Super Empty Hours	0.0744

Notice that it is only considered the active energy price since there is a power factor compensator installed. The only considered tariff is for the Long Usage prices, since the HVAC system is always turned ON. The year quarters column presented in Table 3.1 are the division of the year in trimesters: period I is from January to March, period II from April to June, period III from July to September and period IV from October to December. The correspondence from the schedule time in table 3.1 to daily time is presented in Table 3.2.

Table 3.2: Energy price variation schedule

	Winter time	Summer time
Peak Hours	09.00 - 10.30 h 18.00 - 20.30 h	10.30 - 13.00 h 19.30 - 21.00 h
Full Hours	08.00 - 09.00 h 10.30 - 18.00 h 20.30 - 22.00 h	08.00 - 10.30 h 13.00 - 19.30 h 21.00 - 22.00 h
Normal Empty Hours	06.00 - 08.00 h 22.00 - 02.00h	06.00 - 08.00 h 22.00 - 02.00 h
Super Empty Hours	02.00 - 06.00 h	02.00 - 06.00 h

The time daily schedule for the energy prices varies in the Winter and in the Summer, as the grid demand changes. The shift between both is when Portugal changes from GMT (Winter time) to GMT+1 (Summer time) and vice versa. The energy cost is computed by

$$C_E = \sum_{k=1}^{N} [p_a[q_a(k), t(k)]\ E_a(k)] \tag{3.2}$$

where p_a represents the tariff price of energy for the active power part, q_a represents the year quarter, t represents the time of day and E_a the active energy consumed during sampling period k. Optimizing the energy cost is to minimize the C_E value.

Thermal Comfort

For the thermal comfort objective, the case is rather more complex. In most common standards (ISO 7730 or ASHRAE-55), thermal comfort depends on many factors. Some of them are hard to measure and, at the same time, easy to have its value changed frequently. The calculation method presented in [13] is based on an iterative method, dependent on many variables which were not possible to acquire during the dissertation. However, if some variables are not used, the algorithm may not converge. The alternative is to use a simpler estimator for measuring the thermal comfort.

As a dissertation simplification, the thermal comfort metric is assumed to be just a function of the interior temperature. The influence of temperature on thermal comfort may vary based on human expectation. The temperature expectation is based on many factors, described in [15]. However, there is a simplification, presented on [13], based on a worldwide statistical study, which relates the acceptance interval for temperature with the exterior one. This relation is presented in Figure 3.1.

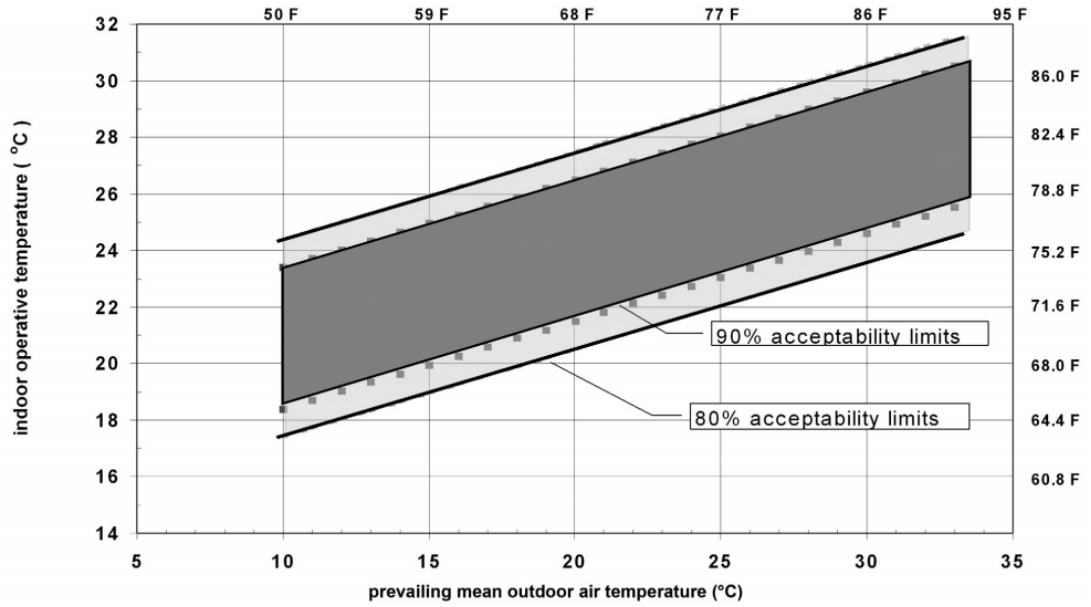

Figure 3.1: Predicted percentage of dissatisfied as a function of exterior temperature [13]

The reference temperature considered, T_{ref}, is calculated with a linear function, parallel to the acceptability limit lines, in the middle of both. As a simplification, this reference temperature is considered to be the expected one. This way, as a first approximation, the instantaneous thermal comfort can be calculated as the absolute difference between the instantaneous temperature and the expected one. The instantaneous thermal comfort is

$$C_{TS}(k) = \min\left\{|T(k) - T_{ref}|\ h_{store}(k), 3\right\} \tag{3.3}$$

where $T(k)$ is the actual temperature inside, T_{ref} is the reference temperature for the room, $h_{store}(k)$ represents the state of the store, either opened or closed, represented with value 1 or 0, respectively, and the value 3 is the saturation chosen. The usage of the store schedule allows an higher flexibility on temperature signal by imposing minor restrictions outside the work schedule from each store. For

instance, during night time, there is nobody inside stores, so, every temperature is considered to have the maximum comfort. The saturation value is based on the thermal sensation scale from the ASHRAE-55 standard, presented in Table 3.3.

Table 3.3: ASHRAE-55 thermal sensation scale [13]

Numeric scale	Sensation scale
+3	Hot
+2	Warm
+1	Slightly Warm
0	Neutral
-1	Slightly Cool
-2	Cool
-3	Cold

For optimization purposes, there is no interest in distinguish hot from cold thermal sensations, just comfortable from uncomfortable ones. Therefore, the absolute value is used, where 0 is the most comfortable case and 3 the most uncomfortable one. That is the reason why the absolute difference is considered in (3.3). In the optimization sense, the thermal comfort estimator must be a value which considers every sample. The expression for the thermal comfort estimator adopted

$$C_T = \text{mean}(C_{TS}) + \text{std}(C_{TS}) \tag{3.4}$$

calculated as a function of C_{TS}. The average of the instant thermal comfort is not a "good enough" estimator for the global thermal comfort, if the period is much longer than the thermal constant. So, it is used the standard deviation, std(C_{TS}). The same reasoning as the energy cost is applied, to optimize the thermal comfort is to minimize the value of C_T.

Diagram

The optimization variable is the chiller setpoint. In (3.2) and (3.3), there is no explicit dependence on the chiller setpoint. However, there is an implicit one, characterized by the HVAC system dynamics. A cost function, for this case, must calculate the objective cost based on the chiller setpoint parameter. Figure 3.2 shows a diagram of the cost function calculations.

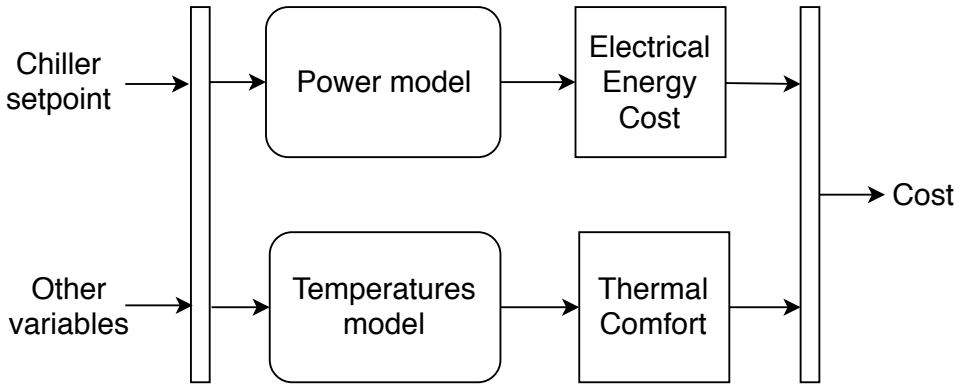

Figure 3.2: Cost function simplified diagram

In fact, for the optimization algorithm to work, the cost only has to be calculated based on the optimization variable. This anticipates the need of two models, presented with round-edge rectangles in Figure 3.2. These models calculate the variables needed for the explicit cost calculation based on the chiller setpoint and other information it may be necessary. The modeling process is based on data-driven models and described in detail in Chapter 4.

3.2 Meta-heuristic Algorithms

Meta-heuristics are mostly based on observed nature behavior in different situations, considered to be effective ones. These optimization methods are best suited for using with data-driven models since the optimization method does not imply the knowledge on the explicit derivative of cost function. This is the case for the formulation presented in Section 3.1. Therefore, this dissertation scope focuses on meta-heuristic optimization algorithms.

All meta-heuristic algorithms have one common base. They start with one initial randomly initialize population with a user-defined size. Every iteration the population evolves through a algorithm-based criteria. It is not granted to be achieved the optimal solution. However, for a good sized population, a near-optimum is often achieved. The final result is selected from the last iteration population, based on a user criteria. The considered meta-heuristics are genetic algorithm and particle swarm optimization.

Genetic algorithms are the most influential meta-heuristic algorithms. They follow the biological evolution principle. Therefore, an algorithm iteration corresponds to a generation and each element of the population to a gene. In every generation, there is a creation of new genes, selection of parent and mutated genes and elimination of genes. The creation of new genes occurs based a combination of parent genes from last iteration, through a combination operation. Other genes suffer a mutation process, altering them. The elimination occurs on worst genes from last generation. In last generation, the best gene is selected as the optimal solution.

Particle swarm optimization follows the biological principle of socio-cognitive learning. It replicates the behavior bird flocking or fish schooling. In this case, the population corresponds to the swarm. In every iteration there is a learning process in all swarm elements, based on three factors. The first factor is the actual inertia on each element actual movement. The second factor is the cognitive learning one, from which the element learns with the local information. Last factor is the social learning factor, from which the element learns from the best positioned element in the swarm. In last iteration, the best swarm element is selected as the optimal solution.

There is no prior reason for one to achieve better results than the other, the performance is case dependent. This dissertation compares the usage of both in terms of obtained results and convergence. On genetic algorithm, it is used the NSGA-III (Non-dominated Sorting Genetic Algorithm) implementation, a reference one considering genetic algorithms. On swarm optimization, it is used PSO (Particle Swarm Optimization), one of the most widely accepted algorithm in swarm optimization. Both used implementations are publicly available in yarpiz website [18].

3.3 Pareto Optimization

A natural conclusion, when dealing with multi-objective optimization, is that after running the algorithm, it is not always obvious the best solution to choose. Using the common meta-heuristics algorithms, in the last iteration of the algorithm there is a set of many solutions from which the best one have to be chosen by a criteria applied afterwards, preferably with the case study in mind.

There are usually 2 steps when selecting the optimal solution. The first step is a common known method called Pareto optimization. This method consists in choosing the points from the solution set which are part of the Pareto frontier. For the minimization on both dimensions case, a Pareto frontier follows a strict mathematical definition

$$Z_p = \{\mathbf{z} \in \mathbf{R}^n : C(z_i') \leq C(z_i), \text{for all } i,\ \mathbf{z}' \in Z\} \tag{3.5}$$

For each point of this frontier there is no other point which improves one of the objectives without deteriorate another one. The final solution considered belongs to this frontier. Figure 3.3 shows the application of the definition in (3.5) on an example population.

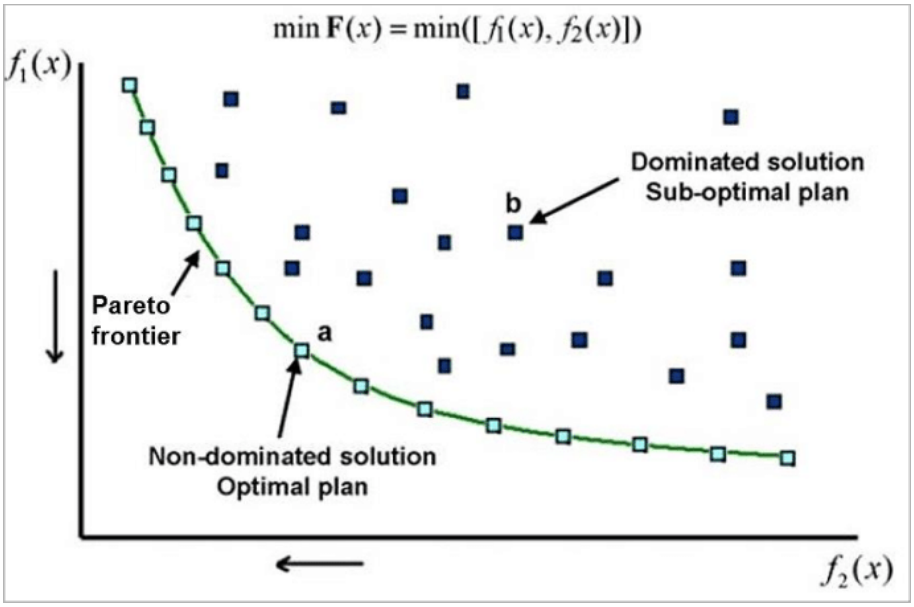

Figure 3.3: Pareto frontier example for minimization of 2-dimensional cost function [19]

The second step is one in which the case study can be taken into account. There is not a general method to choose the best solution from the Pareto frontier. The solution used on Cascais Center case study is described on Section 5.1.2.

Chapter 4

Observers

Chapter 3 presents the optimization cost function definition for the Cascais Center case study. The cost function allows for the objectives cost calculation based on the optimized variable, the chiller setpoint. However, the simplified diagram of the cost function, Figure 3.2, shows a need o for intermediate models for the calculation to be possible. These models are the base for the open-loop strategy, allowing the optimal control framework to be implemented. They are currently referred as observers.

The observers keep the optimization results physically feasible, using dynamics prediction. The prediction models used are based on data-driven models using supervised learning. These observers allow for estimating the influence a chiller setpoint alteration may have in the energy consumption and interior temperature variation. Based on these results, the optimization algorithm can choose the best chiller setpoint for ensuring the balance on both objectives.

During this chapter, it is presented the the main principles of the used observers. This includes information extraction and representation, predictive model selection and implementation of the observers. The results achieved on this implementation are presented at the end of the chapter.

4.1 Data Pre-Processing

The collected data is not usable in its raw state, in which is it acquired. This is intensified by the fact of not having the sensors synchronized with each other and some third-party ones. Other information does not come on a sensor acquired form. In each case, there are needed pre-processing steps in order to make it useful and have the information in a way it can be extracted and used into modeling.

The manual process of configuring sensors, putting it on right location and getting the data have in consequence incomplete day acquisitions at the begin and at the end. Theses days have a small and different number of samples for each day. First step to make post-processing easier is to remove these days in order to create a clean dataset of complete days to extract a complete daily dynamic. The variables are acquired in independent sensors with a necessarily different configuration. The electrical power and interior temperature data were acquired for the purpose of having a 5 minutes sampling period, and the meteorological data were acquired by a third-party entity with a 1 hour sampling period.

The electrical power data and the interior temperature acquired results in a situation roughly similar to the one on Figure 4.1

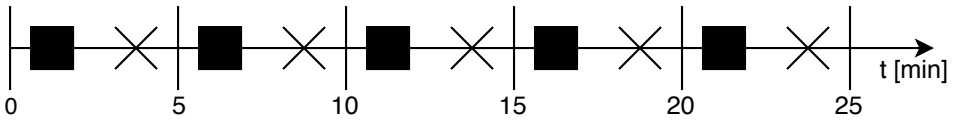

Figure 4.1: Temporal diagram of a data acquisition example

where the square and the cross markers are representing acquisitions of different variables in a time scale. These variables have an non-coincident sampling period despite having the same duration. For modeling purposes, it is important to have coincident sample values for the acquired variables. This is achieved by using linear interpolation.

The linear interpolation process starts by choosing a new sample timetable. This new timetable is fixed to be one considered to be a more convenient one for modeling purposes. The values of the acquired data is not known on this timetable nor its dynamics. Using linear interpolation is to assume that the value between two acquired samples can be described by a linear equation which contains these points. This is a valid approximation considering that the variables have a slow variation when compared with the acquisition sampling frequency. A value calculated with this method is a better one in this new timetable than using the nearest one acquired.

There is some useful information for modeling that was measured by the sensors. Most of this information is related to schedules and routines of people working there or clients there. For instance, there is a lower number of people inside the building during weekends than during working days. Like the other information from the sensors, this one also needs some pre-processing steps, to be in a usable format. On chapter 4.2.3, it is explained the importance of each of these variables. For now, it is presented the process of format conversion on this information into a more convenient one.

There is information related to the commercial activity of both stores directly to be converted to a new format. For each store there is a boolean value on each sample, equivalent to the stores' states *opened* and *closed*. The week day is converted to a variable which can assume 7 states, representing the 7 days of the week. Then, the conversion of HVAC system commands. The schedule from air handlers follow the same format as store schedule with one boolean value for each sample, representing the states ON and OFF. The chiller setpoint have a real number value on each sample.

4.2 Observer Structure

The observer structure defines the sequence of calculations needed for predicting the output based on input information. The structure of the observer includes the predictive model, but may also include some amount of pre-processing, depending on principles of the model. On a dynamical system, the usual differences in between observers are in number of inputs and outputs and the amount of delay on input or previous output information used on each sample prediction.

The outputs are the variables to observe, in this case, the power used and the interior temperatures

on Social Security store and Loja do Cidadão. The inputs are a set of variables extracted from many measurements (the process to do it is presented in 4.2.3). For the power used and mostly for the temperature case, it is mandatory to use information from previous instants. The observers are implemented in two different predictive models, the NARX Neural Network and the Takagi-Sugeno. All the observers implemented are based on a canonical structure which follows these principles in their own structure. The canonical form is presented in Figure 4.2.

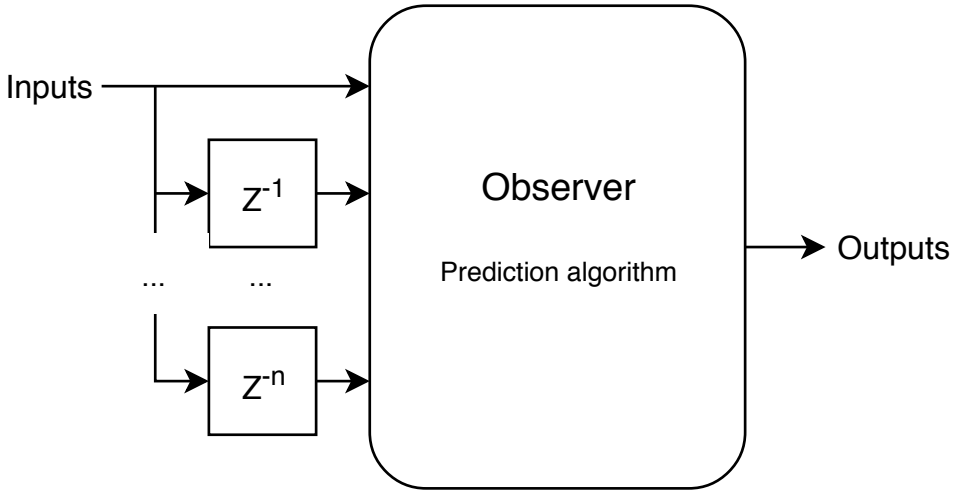

Figure 4.2: Canonical form of the used observers

Notice that Figure 4.2 diagram only shows common characteristics of the different observers implemented. The predictive models may have intrinsic characteristics which add complexity to the diagram.

4.2.1 Operating Mode

Nothing has a bigger impact on HVAC system dynamics than the selected operating mode. The system reacts differently to the environment when it is either heating or cooling. The hierarchy of importance on each part of information extracted is a different one for each operating mode.

The dynamic changes are caused by many factors, either they are directly or indirectly related to it. Many components on HVAC just turn ON on one of the operating modes. As an example, one of the chillers only turn ON on cooling mode. This is particularly important for this dissertation since it causes a huge difference on setpoint sensitivity. One factor which influences indirectly is the weather seasons. For instance, the operation modes are highly correlated to the weather seasons. The weather seasons are indirectly related with the people occupancy inside the stores. For instance, in August, the need to use the Social Security store services decrease. Another example is that in May, when the bathing season starts, there might exist an increase on Loja do Cidadão occupancy. Cascais city has a beach near the capital. Many people which would go to other equivalent stores on other seasons may go to this one during this year season. Notice that it was not possible to acquire this data, these examples are just based on educated guesses.

Two options immediately rise to solve this issue. The alternative of training the observers with an input for the operation mode or training different observers for each. During the dissertation, the alternative

of operation mode as ON or OFF as inputs to the observers showed poorer results than the alternative. This way, for each operating mode, the observers are implemented separately.

4.2.2 Prediction Model

The prediction model is the mathematical model which allows the estimation of a future value based on past and present values, either from the other variables or the variable being observed. The prediction model is a part on the observer canonical structure, presented on chapter 4.2. Therefore, it is needed to choose a data-driven model that can learn from the acquired measurements. The models used for this thesis project are NARX Neural Network (Nonlinear Autoregressive Network with Exogenous Inputs) and Takagi-Sugeno.

The first model is NARX Neural Network, the most widely used model for energy consumption optimization in HVAC systems on state of art scientific papers. It is an enhancement of the classic standard Neural Network model. It supports its improvement in the assumption that the predicted instants have a strong mathematical relationship with previous ones, often the case for dynamical system behaviour. This model often excels in predicting temperature dynamics. The diagram of the NARX model is presented in figure 4.3.

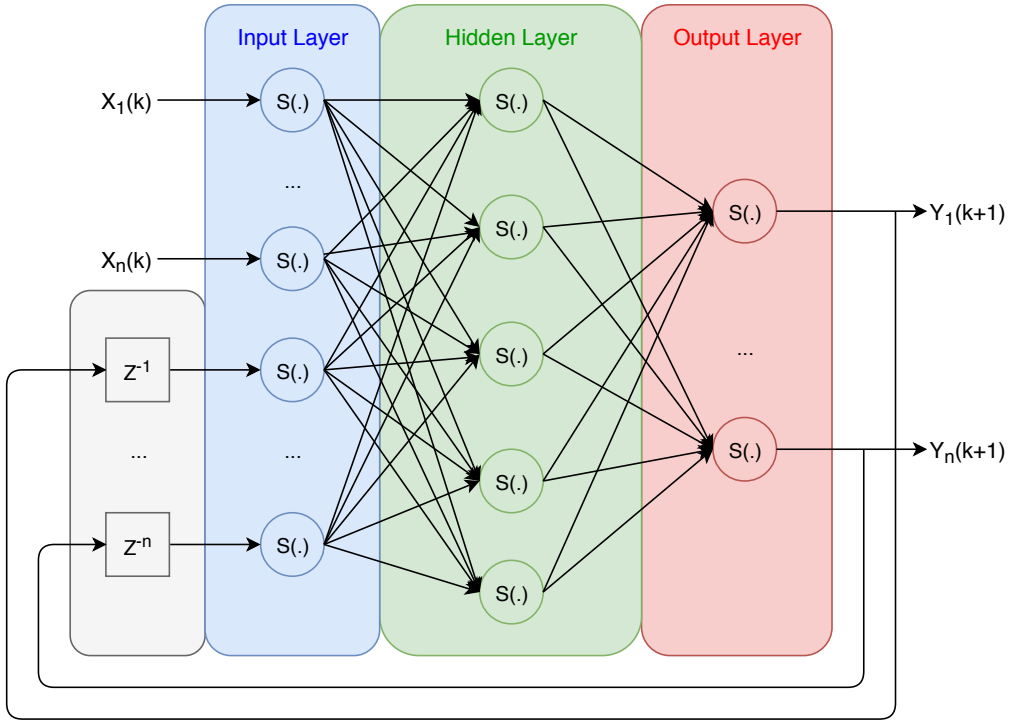

Figure 4.3: NARX Neural Network model diagram

The NARX Neural Network model has 4 different functional parts, represented in the diagram with 4 colored round-edge rectangles. Starting with the model's input variables, there are the external input and the feedback loop inputs for the previous outputs. The external input variables enter the input layer directly. The feedback ones have additional processing, represented in the diagram with a grey rectangle. It can be interpreted has a buffer for the previous predicted values, for making them available

on the right samples' prediction. It is not considered a layer of NARX, but it has an important enough part for me to remember its functional value there. In this Figure 4.3 the delay blocks (represented with $Z^{-m},\ m \in N$) are connecting just one output, but in real case they are connecting every output. This is a tentative to not overload the image with arrows crossing each other. The other rectangles have represent actual layers from the Neural Network, with arrows representing value gain computation and propagation flux and the circles representing the neurons. The neuron makes a sum of all inputs and then it applies the sigmoid function to the result. For the thesis project, the sigmoid function chosen is the standard one

$$S(x) = \frac{e^x}{e^x + 1} \tag{4.1}$$

The input layer provides a gain computation for the inputs of the model. It is like a second order normalization, done on top of all pre-processing. The hidden layer works do an internal product for the previous layer output values, with different weight vectors. The number o hidden layers at NARX is variable and it usually depends on the modeling complexity of the problem. The output layer works mostly the same way the hidden layer, except it has actually the number of neurons equal to the number of outputs.

The used implementation of NARX Neural Network is from a well tested mathematical software. Though, it is highly costumizable, allowing to adjust parameters to the specific case. It is available for user to choose the delay of input variables (external and feedback ones), the sigmoid function, the training algorithm, the performance metric and sets division (this is covered in chapter **??**).

The second model considered is Takagi-Sugeno model. It is used for modeling applications, predicting the produced power on turbines using wind speed data. The choice of this model for this dissertation project was done because the model is more robust to data uncertainty than NARX Neural Network model. This characteristic derives from its initial layer, which uses the fuzzy principle, making a clusterization of input data. This type of observer is implemented with feedback, using previous predicted instant results, and without feedback. The results showed instability, then, only the non-feedback alternative is considered. The diagram of the model implementation is presented in figure 4.4.

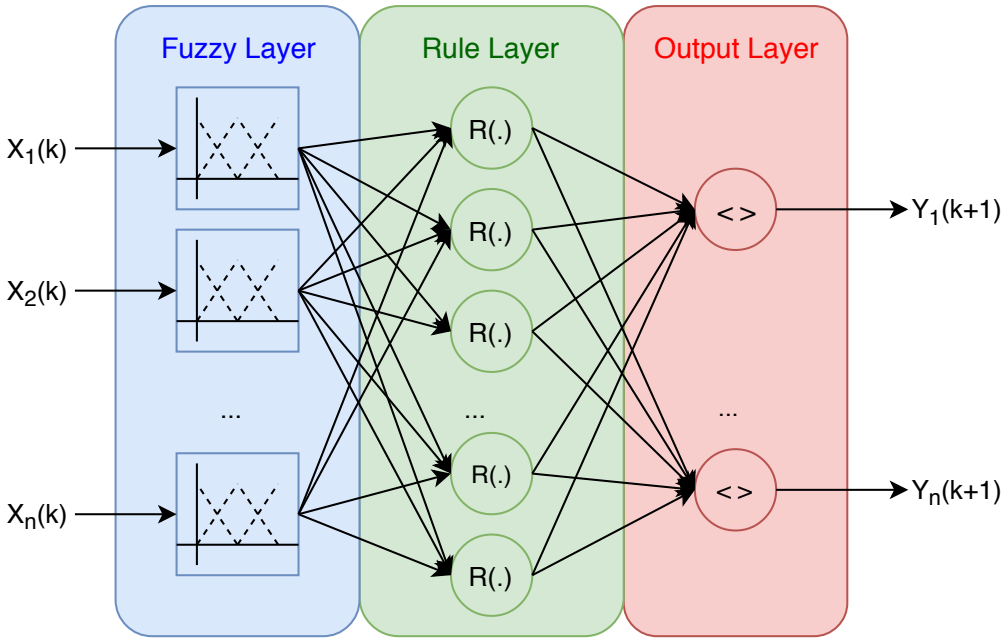

Figure 4.4: Takagi-Sugeno model diagram

Takagi-Sugeno model has 3 functional parts, represented with 3 colored rectangles. The fuzzy layer is the equivalent to the input layer in NARX Neural Network case. For every input, it is applied a fuzzy inference, which is a type of clusterization. This process is done through the membership function which can be one of many. The rule layer is commonly referred as hidden layer and it has an equivalence to the layer in NARX Neural Network. Here it is referred as rule layer in order to avoid confusion, as it has a high functional difference. In this layer, there is the same concept of neuron, however, all the input weights are 1. The input variables in this layer's neurons are multiplied instead of summed up. At neuron's output an activation operation, in here referred as rule, which can be either AND or OR operation on the variables. The output layer makes the defuzification operation. The defuzification operation chosen in here is base on the center of mass operation.

$$Y_n(k+1) = \frac{\sum_{m=1}^{M} w_m r_m(k)}{\sum_{m=1}^{M} w_m} \tag{4.2}$$

where w_m is value index m of weights vector, r_m is the output index m of rule layer and M the number of neurons output layer.

The used implementation of the Takagi-Sugeno model was developed for the thesis project work, using a mathematical software. The implementation is done in a way that allows the usage of custom features. As an example, an input delay implementation is not part of the Takagi-Sugeno model itself, but an important feature in this project's observers.

For both observer models, there are some diagram simplifications to be noticed, made to simplify their comprehension. The prediction of a variable in sample $k+1$ can depend on more than one previous samples instants. The prediction of sample $k+1$ can depend on k, $k-1$, ..., $k-n$ sample inputs. The same can be applied on NARX Neural Network for the output feedback. The decision is made based on an analysis of if adding a previous sample and increasing its complexity have a good enough advantage

in modeling performance. Further, this analysis is done for the real data on chapters 4.4.2 and 4.4.1.

4.2.3 Input Variables

The number of used variables is high and they have redundant information, mostly because meteorological data is redundant itself. Besides that, the signals measured represent physical variables from different kinds, so they have different ranges of values. These facts usually lead to an over-fitting process in training and/or a worse performance behavior from the observer. The first challenge for good observers modeling is a good set input variable choice.

The input variables are chosen by the quantity and quality of information which can be extracted to describe system dynamic behavior. Some relations are obvious, known from physics, and may even add redundant information. For instance, an increase on solar radiation can cause directly an increase on exterior temperature. Others are less obvious, but just as important, introduced by a process of trial and error. A more intuitive way to think is to choose them by broader fields of behavior. For this dissertation the chosen fields are meteorological data, to characterize dynamics related to the weather variations, routine data, to characterize the ones related with people schedules and some typical client behavior and system command, to characterize the user configuration input. The better it is characterized each field, the better the total. Notice these variables have non-linear relations with each other, adding one new variable may help to provide a better comprehension of another. The process for choosing the inputs is summarized in Table 4.1.

Table 4.1: Considered variables criteria on information extraction process

Variables	Reason
Characterize meteorological environment	
Exterior temperature	Exterior temperature is directly related to the needed energy for maintaining the desired temperature in each part of system.
Solar radiation	The solar radiation is an image for predicting future heating on both interior and exterior temperature.
Humidity	Humidity is one of the most important variables for the human thermal comfort. It can describe also part of HVAC system's fluid behavior.
Wind speed	Wind speed can have influence on system thermal dynamic, mostly on Winter, since a major part of it is outside on the roof. Also, some of the visits to the building showed some store windows opened.
Characterize human routines	
Time of day	The time of the day can be rough estimation to the usual store occupation, mainly when combined with other variables such as week day.
Week day	The week day is the most important variable in characterizing the main routines from stores. It includes information about cyclic behavior, typical from commercial places. This cyclic behavior includes information like differences on daily dependent attendance or clients preferred days.
Store schedules	The store schedule is a boolean variable for each store with states open and close. It is important in predicting more accurately the dynamic differences between stores, due to their different schedules.
Characterize HVAC system commands	
Chiller setpoint	The chiller setpoint is the user defined temperature for the fluid chiller used on chiller. It is the optimized variable.
Air Handler schedules	The air handler schedule is represented by a boolean variable for each of them, with ON and OFF states. These schedules influence on the degree of chiller action on temperature and evolution of energy consumption.

Notice that there are some fundamental differences in these fields. The meteorological variables field is based on acquired data on physical variables where it is applied a small amount of processing made later. On the human routines characterization, the process is a different one. The information is extracted from some known variables which usually have a direct influence on the human routines. But these are just indirect measurements from which it is possible to induce some amount of the real dynamic. The HVAC system commands field doesn't characterize an environment part. It describes the configuration a maintenance team can alter to adapt it to the building environment. In this dissertation, it describes the configuration which can be optimized.

The variables have different ranges of values. It might be as important information to extract a variation of 0.1 on one of them as of variation of 10 on another. Using the original ranges may lead to information loss because the values of some are neglected when compared to the ones of others. This is solved by normalizing them to a range of [0,1]. The original variables have a lower and an upper bound values are based on original ranges, introduced for the normalization to be possible, presented on Table 4.2.

Table 4.2: Normalization limits for the considered variables

Variables	Minimum value	Maximum value
Time of day [HH]	0	24
Exterior temperature [^{o}C]	0	50
Solar radiation [W/m^2]	0	1000
Humity [%]	0	100
Wind speed [km/h]	0	75
Day of the week	1	7
Interior temperature [^{o}C]	15	35
Store schedule [Close/Open]	0	1
Hot chiller setpoint [^{o}C]	35	45
Cold chiller setpoint [^{o}C]	5	15
Air handlers schedule [OFF/ON]	0	1

Taking into account the chosen variables, presented on Table 4.1, the inputs have dimension 12. Not all of them add the same amount of information and many of them add redundant one, specially inside the same field. In dissertation, it is used Principal Component Analysis algorithm (PCA) in order to reduce dimension. The methodology bases its principle in replacing the actual signals by others, named principal components. These signals have the particularity of describing an equivalent system with an equal or smaller dimension. The higher dimension used, the more information is maintained from the original signals. In this case, the original dimension is 12, since that the store schedule signal has dimension 2 and the air handler schedule has dimension 3. The dimension after applying the algorithm is chosen based on a compromise between the amount of information needed to preserve and the complexity of the resulting observers. The relation between the number of principal components used and the amount of information preserved is shown on Table 4.3.

Table 4.3: Percentage of system behaviour explained by principal components

Number of principal components	Percentage of heat system behavior explained	Percentage of cool system behavior explained
1 component	55%	54%
2 components	73%	71%
3 components	86%	85%
4 components	92%	91%
5 components	96%	96%

The PCA algorithm is, also, applied individually for heating and cooling operating modes. The variables which have more important information for both situations are not the same. As an example, the solar radiation is a much significant variable in the Summer time and the wind speed is much significant in Winter time. The principal component vectors are calculated using information of each period.

The number of chosen principal components can be either 3 or 4, based on Table 4.3, depending on further result analysis. There is not an ideal minimum percentage to choose, it depends on data quality, on desired performance and on accepted error tolerance. The decision is taken after considering the result differences on observers.

During dissertation, the observers presented the best results with 3 principal components. Hence, the input for the observers is constituted by 3 principal components, to characterize the meteorologi-

cal and human routine information, and the normalized command variables, making a total of 7 input variables.

4.3 Dataset Partition

When using supervised learning on different models, there is usually a training set, a validation set and a test set. This division can be done in a way where the training is blind to the data (not considering the particularities of this case) or considering some prior information, based on a prior data analysis, allowing to choose better how sets can have the higher number of different cases.

One widely used way to divide the sets is to randomly choose the samples for each set. This is a poor performance method when modeling dynamical systems, since their dynamic depends on previous sample values. Often, the used method is a three block partition, being the most common division 70% for training set and 15% for validation and test sets. Then it is applied the cross-validation method, variying the partition division. After measuring performance for different partitions, it is calculated an average performance of tested partitions, which is usually considered to be the real performance of the observer.

As a rough approximation, the meteorological cycle can be assumed to have a year period and the routine one a week period. The acquirement periods had durations between one and two weeks, a small duration when compared to both cycles, the routine cycle and the meteorological cycle. It is probable to exist an information gap on system dynamics, since many situations are not on data. At the same time, there are some dynamics which appear rarely on data. However, these cases are important ones to model the system. Using one of the traditional methods for partitioning could lead to a skew training of the observers. For this reason, the division is done based on criteria, defined of prior information on the case.

There is some prior information based on common sense knowledge. For the meteorological data, having the most different cases means to have data from different periods of the year, including if possible the most characteristic month of each season in every set. For the routine prior information, having most different cases means to having cases of different days of the week in every set. Notice that the dynamic of routine data is mostly cyclical with one week period. Despite the custom partition, it is maintained the ratios of 70% for training set and 15% for validation and test sets. In Table 4.4, it is presented an ilustrative example of one possible partition of data with very similiar characteristics to the one measured in Cascais Center. This example dataset has 2 complete weeks from months MM1 and MM2 in year YYYY, making a total of 4 weeks. The blue rectangles represent the days chosen for training set, the green ones for the validation set and the red ones are from test set.

Table 4.4: Dataset partition example

	MM1-YYYY		MM2-YYYY	
	Week 1	Week 2	Week 1	Week 2
Monday				
Tuesday				
Wednesday				
Thursday				
Friday				
Saturday				
Sunday				

Considering the rotine characterization, the two most different days are Saturday and Sunday. These days are present on training, validation and test. All sets have an equitative division between both months. When there are two days of same set in the same week, they were selected to be consecutive, since the observer bases itself on previous data. Based on these criteria, there are many possible configurations, being one of them the one presented in Table 4.4. For the thesis case, there are two different datasets (one for heat and one for cooling). Another criteria considered is to have days with different setpoints on every sets.

This method prevents a certain amount of bias in supervised learning process. It is possible for this case due to a good knowledge of the data, but often not possible for many machine learning applications. There is knowledge of the conditions in which the measurements were taken and also a prior knowledge of some routines in Cascais Center. The partition done on real data is presented on Appendix B.

4.4 Observer Implementation

In previous chapters, the function and main implementation principles of the observers are described. In summary, the observed variables are the power used by the HVAC, the interior temperatures on Social Security store and Loja do Cidadão. All observed variables need two observer implementations, one for heating mode and another for the cooling mode.

The main steps followed during the implementation of the observers are presented in this chapter. This includes considerations in observer structure, supervised learning method, performance evaluation and associated results.

4.4.1 Power Observer

The power observer predicts the power usage of the HVAC based on scenario variables, which describe environment conditions, and the user input configuration. The value of each sample is the average power usage during one sampling period, making it possible to calculate the energy consumption during the interval based on a gain operation. Notice that the air handler from Loja do Cidadão is not included because it was not possible to acquire data from there (see Section 2.4).

Diagram

The power observer aims to predict the HVAC power signal based on extracted input information. The input variables include scenario variables, and others to the user input. In Figure 4.5 it is presented the diagram of the power observer for both prediction models.

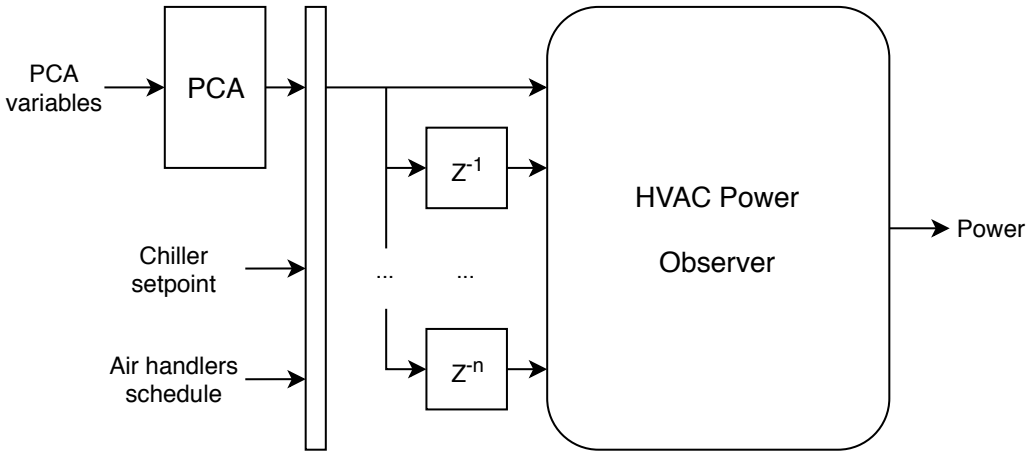

Figure 4.5: Power observer complete diagram

The power in each sample is the average value during the sampling period. The energy consumption during a sampling period can be calculated by multiplying the average power by the sampling period. The observer power instead of energy because the power values allow for faster checking on results by comparing with the HVAC nominal power. The power prediction can be used to predict energy consumption.

Training Process

The NARX Neural Network has 5 hidden layers. The weight initialization is a random one. The training method used was Levenberg-Marquardt, with the MSE (Mean-Squared Error) for measuring training performance. On Figure 4.6, it is presented the evolution of MSE value for each set during the training process.

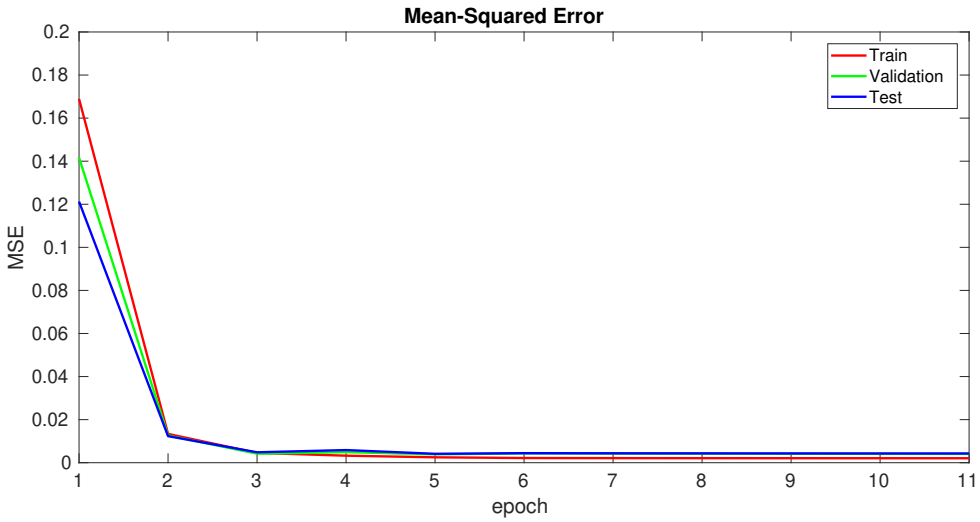

Figure 4.6: MSE evolution for training epochs on NARX observer for cooling operating mode

The Takagi-Sugeno observer training is based on gradient method, using momentum acceleration. The error measure is the RMSE (Root Mean Squared Error) value. The weights are initialized to 0.1. On Figure 4.7, it is presented the evolution of RMSE value for each set during the training process.

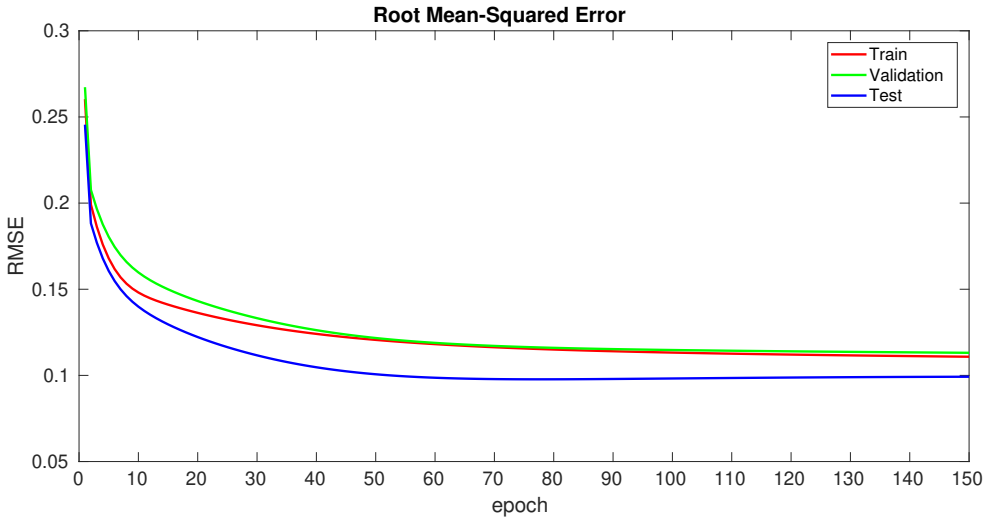

Figure 4.7: RMSE evolution for training epochs on Takagi-Sugeno observer for cooling operating mode

For both methods the epoch in which the results are the best for the validation set is the chosen one for the final prediction model. At NARX Neural Network, the convergence happens with a smaller number of epochs. This may be due to the use of the Levenberg-Marquadt instead of gradient descent.

Performance Metric

Though the power observer predicts average power usage, the real objective in implementing it, is to predict energy consumption and its associated costs. This is arguably the same since the energy can be calculated by multiplying the average power during a sampling period by the sampling period. Notice

that, since the energy costs vary with time, it is important to know the time-point of each sample. The power evolution is not possible to train in models described on previous chapters (see chapter 4.2.2).

One thing to notice is that the variation of the price is slow in comparison with the sampling frequency. Therefore the predicting performance on power observers are based on how well they predict the energy consumption and the associated energy cost. These metrics are applied on observers for both predicting models and presented in Tables 4.5 and 4.6.

Table 4.5: NARX observer results table

Operating Mode	Variable	Real Situation	Observer Prediction	Error
Heating	**Energy [kWh]**	36777	37128	0.96%
	Cost [€]	353.26	354.92	0.47%
Cooling	**Energy [kWh]**	34535	35377	2.44%
	Cost [€]	340.62	339.72	-0.26%

The real and predicted energy and energy cost are compared on test set for both operating modes. The errors show a good adaptation to data on test set. As expected, the errors are higher on energy than on cost, due a slower variation when compared to the sampling frequency.

Table 4.6: Takagi-Sugeno observer results table

Operating Mode	Variable	Real Situation	Observer Prediction	Error
Heating	**Energy [kWh]**	36777	41079	11.70%
	Cost [€]	353.26	395.87	12.06%
Cooling	**Energy [kWh]**	34535	44134	27.79%
	Cost [€]	340.62	425.04	24.78%

Based on the results from Table 4.6, the observer using Takagi-Sugeno prediction model is not able of correctly of predicting the the energy consumption on the HVAC.

On both prediction models, the results are better on heating mode than on cooling mode. One reason is that on on heating mode data, there is a smaller variety of different situations than on the cooling mode. The 27 days on heating mode data are divided in two different months with 3 different chiller setpoints. The 30 days on cooling mode were acquired on 3 different months of the year in two different weather seasons. During these acquisitions, 4 different chiller setpoints were tested. Another reason is that the cooling mode depends less on the setpoint considered, since the second chiller may be working in parallel during this time, mainly during Summer.

Chiller Setpoint Sensitivity

The sensitivity to the chiller setpoint variation is an influential result on the observer performance considering this dissertation. The chiller setpoint is defined as the optimized variable, the altered one in order to optimize the HVAC. The number of different chiller setpoints tested during the data acquirement is a small one in a small range of variation. Therefore, a good performance on test set does not imply a good extrapolation for setpoints outside the range available in dataset.

For evaluating the chiller setpoint extrapolation, it is chosen a typical day, from which the results are compared. On Tables 4.7 and 4.8 it is presented the variation on the energy consumption and cost

predictions for different chiller setpoints.

Table 4.7: NARX Neural Network power observer sensitivity to chiller setpoint

Heating			Cooling		
Setpoint [^{o}C]	**Energy [kWh]**	**Cost [€]**	**Setpoint [^{o}C]**	**Energy [kWh]**	**Cost [€]**
35.0	15515	148.64	05.0	5283	51.17
37.5	10399	101.03	07.5	5524	53.35
40.0	5102	49.27	10.0	9625	93.43
42.5	7740	75.44	12.5	9626	94.54
45.0	5210	50.08	15.0	9426	94.29

The cost sensitivity to the chiller setpoint variation shows a behavior opposite to the expected one in Table 4.7. For the heating mode, the cost is expected to increase when the setpoint increases. On cooling mode, the expected is for the cost to increase when the setpoint decreases. This is possibly a result of a bad modeling extrapolation for other setpoints, not present in the dataset. The cooling mode shows a more notorious example of the situation described. There is a cost step evolution on middle range values and a saturation on values around the frontier setpoints.

Table 4.8: Takagi-Sugeno power observer sensitivity to chiller setpoint

Heating			Cooling		
Setpoint [^{o}C]	**Energy [kWh]**	**Cost [€]**	**Setpoint [^{o}C]**	**Energy [kWh]**	**Cost [€]**
35.0	6320	60.94	05.0	8674	84.33
37.5	6242	60.19	07.5	8843	86.04
40.0	6418	61.90	10.0	8763	85.18
42.5	6895	66.46	12.5	8453	82.16
45.0	6451	62.20	15.0	8526	82.88

On Takagi-Sugeno power observer the tendency is the same. The sensitivity of the energy consumption to the chiller setpoint variation does not follow the expected variation. For both cases, there does not seem exist such an influence of the chiller setpoint on prediction value.

4.4.2 Temperature Observers

The temperature observers predict the temperature evolution for the thermal zones described on chapter 2.2. Their function is to predict the temperature based on scenario variables, which describe the environment conditions, and the HVAC input configuration. There are two temperature observers, one for each store. The temperature evolution is needed for the thermal comfort calculation.

Diagram

Two temperature observers are used to predict three different temperature signals, from the chosen thermal zones. One of the observers predicts the ambient temperature at the Social Security store. The other observer predicts two temperature signals from Loja do Cidadão thermal zones: the fan output one and the ambiance one. Figure 4.8 presents the diagram of temperature observer of Social Security store.

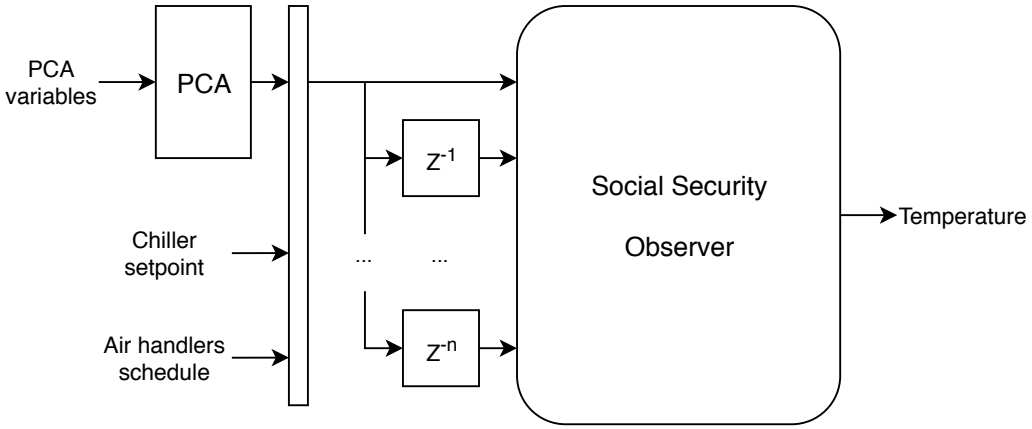

Figure 4.8: Temperature observer for Social Security store complete diagram

In Loja do Cidadão, there are two thermal zones, resulting in two different temperature signals to predict. These temperatures share common dynamics and causality effects from one to the other. Fo instance, the ambiance temperature follows many dynamics of the output one, with different intensity and time delay. Therefore, both are predict by the same observer, following the approach presented in [11]. In Figure 4.9 it is presented the diagram of temperature observer for Loja do Cidadão.

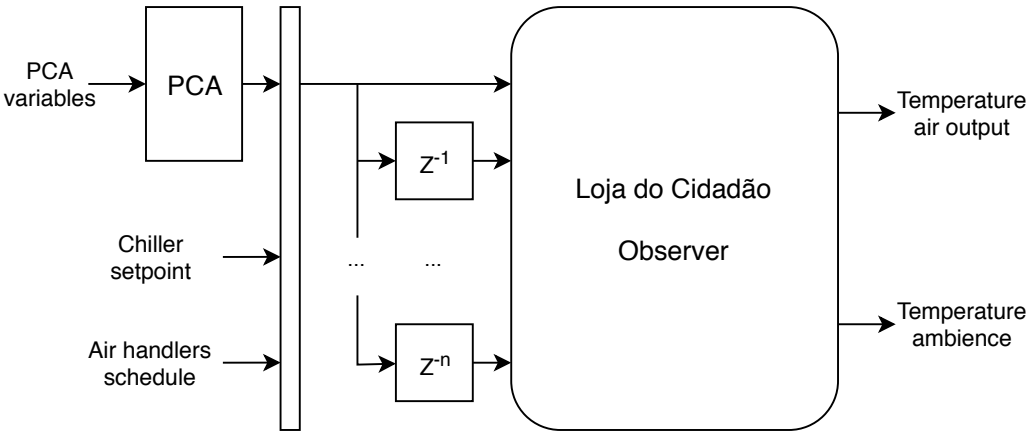

Figure 4.9: Temperature observer for Loja do Cidadão complete diagram

The observers from different stores are trained separately since their temperature is controlled on different air handlers. Different air handlers imply a different temperature reference in the room, controlled separately. During dissertation, this approach showed better results.

Training Process

The NARX Neural Network has 8 hidden layers. The weight are initialized randomly. The training method is Levenberg-Marquardt, with the MSE (Mean-Squared Error) for measuring training performance. On Figure 4.10, the evolution of MSE value for each set during the training process is presented.

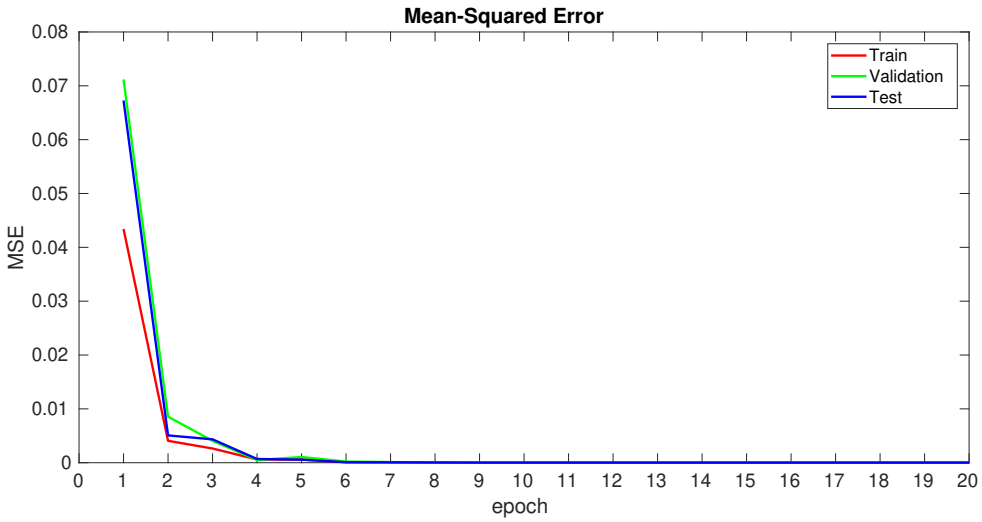

Figure 4.10: MSE evolution for training epochs on NARX temperature observer of Social Security store for heating operating mode

The Takagi-Sugeno observer training is based on the gradient method, using momentum acceleration. The error function use is the RMSE (Root Mean Squared Error) value. The weights are initialized to 0.1. On Figure 4.11, it is presented the evolution of RMSE value for each set during the training process.

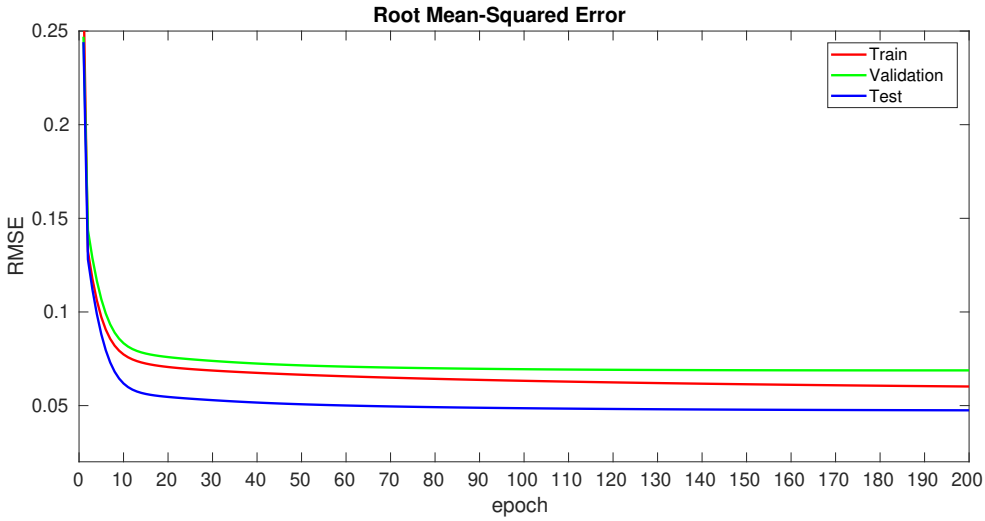

Figure 4.11: RMSE evolution for training epochs on Takagi-Sugeno temperature observer of Social Security store for heating operating mode

For both methods, the final prediction model is chosen according to the validation set error. More specifically, the model from the epoch which has the smallest validation error. Similarly to power observer case, at NARX Neural Network, the convergence happens with a smaller number of epochs. It may be direct consequence of the use of the Levenberg-Marquadt instead of gradient descent.

Performance Metric

To evaluate the performance of temperature observers, a set of empirically metrics were chosen. These metrics allow for a simple comparison of results on multiple observers. These are AAE, average absolute error, ESTD, error standard deviation, and MAE, maximum absolute error. The metrics are calculated based on error from test set of heating and cooling operating modes (see Section 4.2.1). The values are presented in absolute value in ^{o}C and on percentage of the normalized value to the temperature of 25^{o}C. The implementation results are presented on Table 4.9 and 4.10 for both prediction models.

Table 4.9: Performance metrics for Social Security store temperature observer

Metric	NARX Neural Network				Takagi-Sugeno			
	Heating		Cooling		Heating		Cooling	
	[^{o}C]	[%]	[^{o}C]	[%]	[^{o}C]	[%]	[^{o}C]	[%]
AAE	0.94	3.74	1.11	4.45	1.06	4.23	1.23	4.93
ESTD	0.91	3.64	1.33	5.34	1.03	4.10	1.69	6.76
MAE	2.66	10.66	3.35	13.40	3.33	13.33	5.13	20.52

The standard deviation is in the same order of magnitude as the average value. For every observer, the maximum error is one order of magnitude above the average error. This shows poor modeling performance on some dynamics. For the observers from Loja do Cidadão, the result is presented for each predicted temperature individually on every metric.

Table 4.10: Performance metrics for Loja do Cidadão temperature observer

Metric	NARX Neural Network				Takagi-Sugeno			
	Heating		Cooling		Heating		Cooling	
	[^{o}C]	[%]	[^{o}C]	[%]	[^{o}C]	[%]	[^{o}C]	[%]
AAE	1.09	4.37	1.30	5.21	1.28	5.13	1.07	4.30
	1.13	4.52	1.25	4.99	1.43	5.73	1.04	4.46
ESTD	1.29	5.17	1.40	5.61	1.44	5.78	1.08	4.32
	1.41	5.65	1.53	6.12	1.67	6.68	1.12	4.46
MAE	3.15	12.60	2.03	8.13	4.28	17.13	3.08	12.33
	3.48	13.93	3.67	13.68	4.49	17.97	4.06	16.25

For the Loja do Cidadão observer, the same conclusions form the Social Security observer can be taken. The standard deviation error has the same order of magnitude as the average error and, often, an higher value. The maximum is, at least, the double of the average error for every observer. This result demonstrates a poor modeling temperature dynamics.

Every NARX Neural Network observer showed a better performance when compared to the Takagi-Sugeno for the same variable prediction. Though, the maximum error in the observers is to high for them to be considered as good observers. The pattern on the chosen metrics is a characteristic one of an observer with non-modulated dynamics. Taking as an example the NARX Neural Network observer for Social Security store on cooling mode, an AAE of 4.45% may be considered a good value. It shows the average order of magnitude on temperatures is well learned. However, having an ESTD of similar value shows for many dynamics not followed, in a way that for worst sample the error is 13.40%. Perhaps, for specific samples where there may be lack of information.

Chiller Setpoint Sensibility

The sensitivity to the chiller setpoint is another important characteristic in temperature observers. The objective in doing this is the same as before, to better understand the impact of not having data for all the chiller setpoints when modeling. To reduce the complexity of the analysis, only the sensitivity on temperature observer of Social Security store. Since the types of dynamics which influence the temperature evolution are similar ones for both stores, the analysis made for Social Security observer give a good enough intuition of the temperature observer of Loja do Cidadão.

The followed strategy is the same as in power observers case. There is one chosen day (the same days as before) for each operating modes in which different setpoints are tested. The results are shown on both types of observers, the NARX Neural Network and the Takagi-Sugeno, and compared. In Figure 4.12, the prediction on temperature signal during one day for different constant setpoints on heating operating mode is presented.

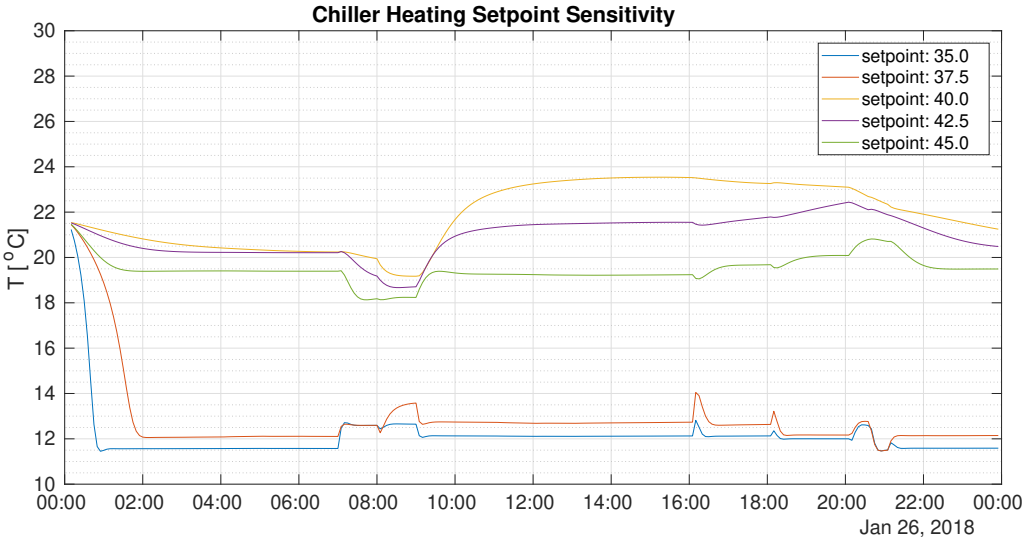

Figure 4.12: Predicted temperature signals for different setpoints during an example day heating mode using NARX Neural Network

Notice that the temperature starts at the same point on every setpoint. The reason is that NARX Neural Network model strongly depends upon previous instants, which were the same for all simulation results. In Figure 4.12, the increasing of the setpoint does not always correspond to an increase in temperature, as it would be expected. For instance, for the setpoint of 45.0^{o}C, the temperature is always lower than for the 40.0^{o}C. This happens for setpoints which are not a part of dataset, showing that the dynamic is not well modeled for them. For the lower values of chiller setpoint (35.0 ^{o}C and 37.5^{o}C), the temperature shows an unexpected dynamic. It shows an horizontal line in every part of day except around the open and close actions on both stores and on the parts of day in which the air handlers turn ON and OFF. Though it would not be compatible with the heating operating mode. To better understand it, Figure 4.13 shows the exterior temperature during the same day.

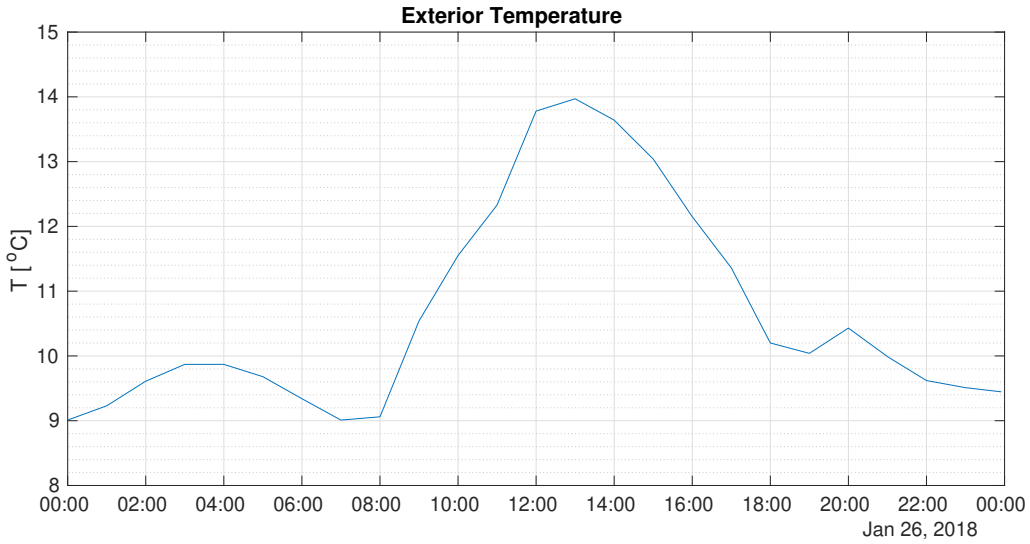

Figure 4.13: Exterior temperature during January 26 of 2018

Looking at the exterior temperature, it is easy to identify samples in which the interior temperature is lower than the exterior one for the referred setpoints. This dynamic is not compatible with the heating operating mode. The same simulation is presented for the cold operating mode on Figure 4.14.

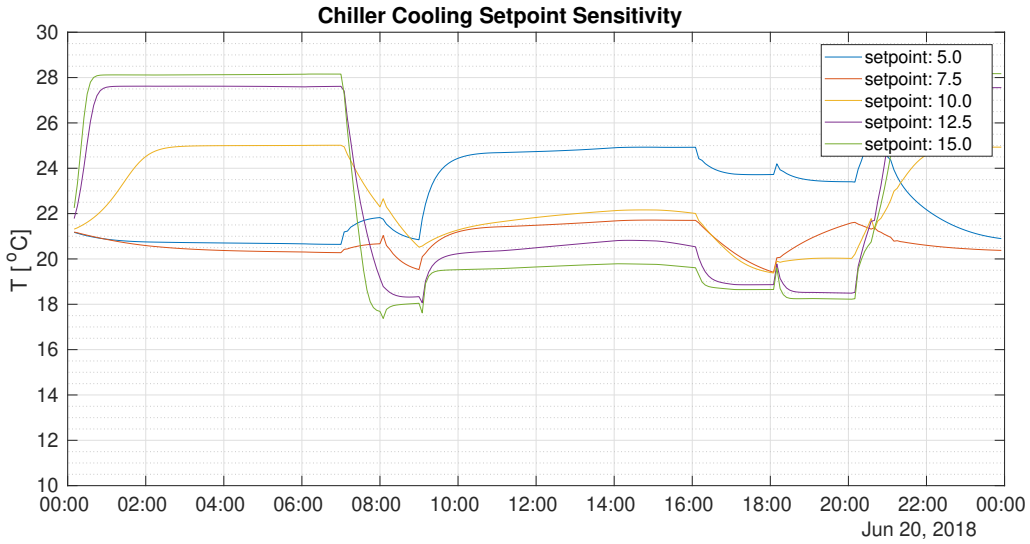

Figure 4.14: Predicted temperature signals for different setpoints during an example day cooling mode using NARX Neural Network

In Figure 4.14, the decreasing of the setpoint does not always correspond to a decrease in temperature, as it would be expected. For instance, during a considerable part of the day, the temperature on setpoint of 5.0^{o}C is the highest value. The Figure 4.15 presents the exterior temperature during the same day.

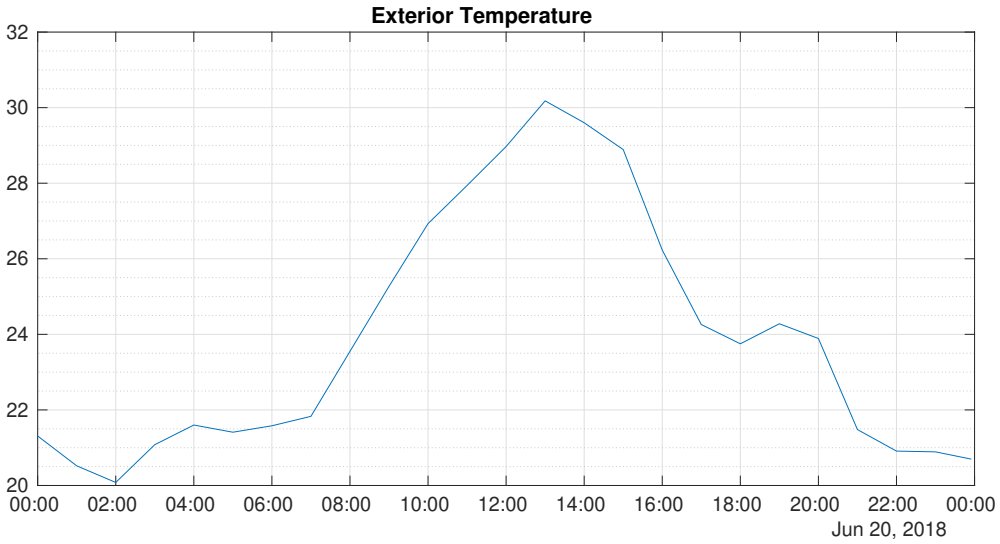

Figure 4.15: Exterior temperature during June 20 of 2018

It makes sense for the temperature to go down during the period in which air handlers are turned ON. But is does not make physical sense to go higher than the exterior temperature, during night and with the store closed.

On both cases, it can be noticed that on setpoints which are part of the dataset, the dynamic result is much more coherent with the schedules from stores and air handlers and the outside temperature. Many of the tested setpoints are not included in the acquired data. The influence of exterior meteorological variables is not well modeled by the observers. This issue gets more evident if the considered setpoints are outside of scope of the acquired data.

For the Takagi-Sugeno model, it was applied the same method. Again, the same days are considered to compare the evolution on the temperature inside Social Security store on different setpoint values (the same values as before). On Figures 4.16, it is presented the interior temperature on Social Security store during a day for different setpoints on heating mode.

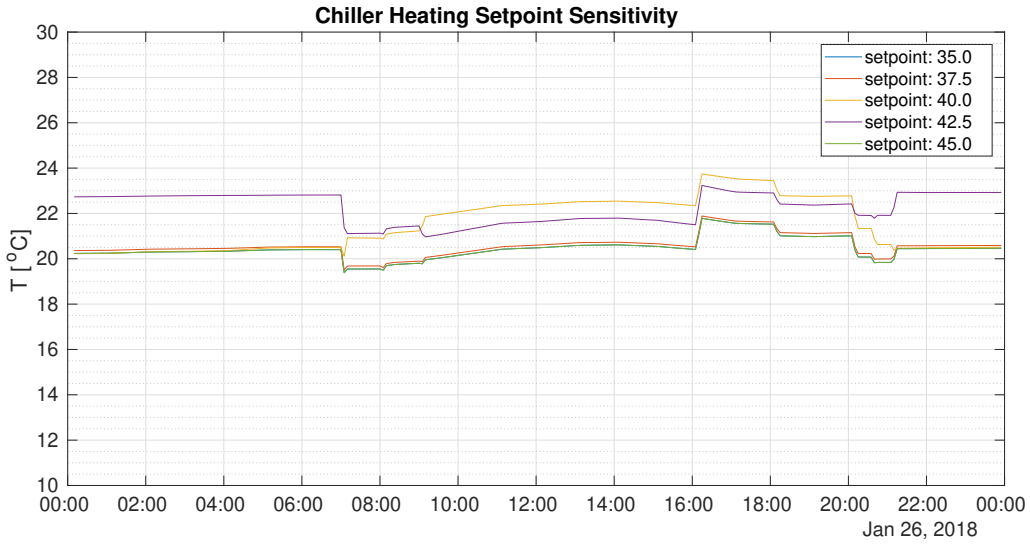

Figure 4.16: Predicted temperature signals for different setpoints during an example day heating mode using Takagi-Sugeno

The results obtained on Takagi-Sugeno are similar to the ones obtained for the NARX observers when it comes to chiller setpoint sensitivity. It is not clear the effect of the setpoint on temperature. For some setpoints, the temperature overlaps, which shows that the modeling differences are small ones. An higher setpoint does not necessarily imply an higher interior temperature. At this point, there is no clear dynamic that should be directly excluded like it is on NARX observer. Despite that, an interesting result is that the setpoint does not alter the shape of the signal. The setpoint acts as an offset to the temperature signal, increasing or decreasing the same value in all samples. This result, despite being coherent, is not coherent with an highly non-linear system. In Figure 4.17, the interior temperature on Social Security store during a day for different setpoints on cooling mode is presented.

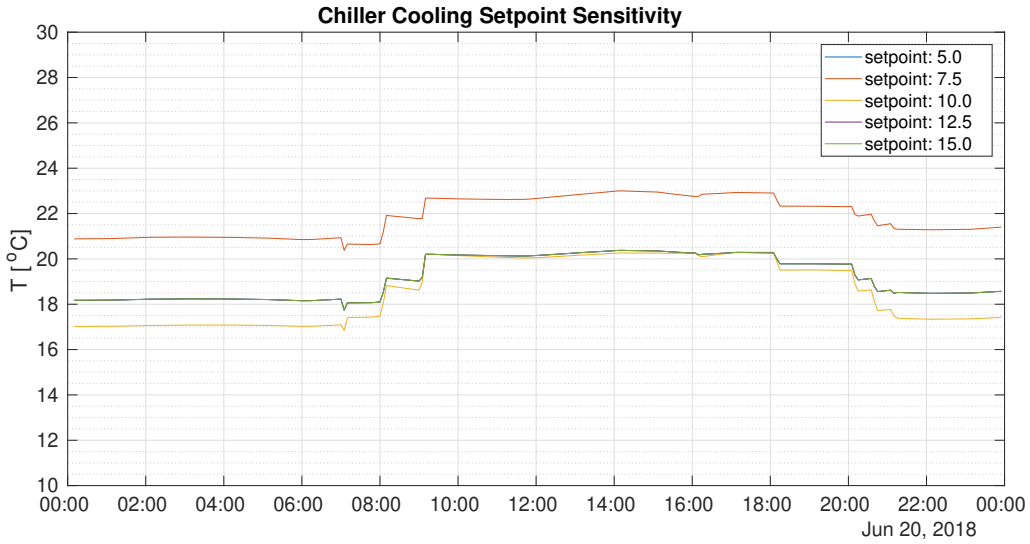

Figure 4.17: Predicted temperature signals for different setpoints during an example day cooling mode using Takagi-Sugeno

On cooling mode, there is an higher number of overlapped signals than on heating mode. The same

conclusions taken from the heating case can be taken here. There is no clear relation of the setpoint with the resulting temperature and changing it just adds or subtracts a signal offset.

Chapter 5

Optimization and Observers Integration

Previous chapters presented the optimization method and the observers separately. However, the optimal framework is dependent on the integration of these systems. This process is not as trivial as it may look. Remember that every result presented on next chapters depends on performance of every module described before, but also on how the integration is done.

In every result presented, there is a definition of as optimization scenario. An optimization scenario is the set of conditions which influence the optimized chiller setpoint, based on the considerations done already. It includes the operating mode and the input variables in observers which are not optimized variables. In this case, it includes every input considered, except for the chiller setpoint.

This Chapter presents the considerations done for having the integration on both systems. Notice that many of the decisions presented in this Chapter could be different ones on a different case study, with a different environment. For instance, a definition of an optimization scenario or a method to choose a Pareto solution applicable to the Cascais Center case may not be applicable in a different situation.

5.1 Optimization Structure

The optimization process allows for choosing a chiller setpoint for minimizing both objectives cost function. The implementation uses different observers on both operating modes, heating and cooling, and defines different upper and lower bounds for the optimized variable, corresponding to the limits accepted for the chiller setpoint in each case. Due to constraints occurred during dissertation, it focuses on the hybrid chiller setpoint, the one which allows heating and cooling operating mode.

The optimization process considers a constant value for chiller setpoint during one week, starting on a Monday and ending on a Sunday. It corresponds to the period of the commercial routine cycle of 1 week. The period is chosen based on a compromise to have weather forecast values with smaller error margins as well as avoid the cost associated with the transient behaviors when changing the setpoint. These costs are not taking into account on the optimization since the observers do not model

this dynamic. The optimization results are, only, presented in Chapter 6 using the NARX Neural Network observers. These implementations showed better performance on the objectives for every scenario.

This Section presents the considerations during integration of the optimization and observers, respecting the principles described in previous Chapters. Many options are more related with implementation issues and considerations for it to be applied in Cascais Center case study.

5.1.1 Cost Function

The chiller setpoint does not directly relates with any of the objectives. Instead, it changes the dynamic of the HVAC, which influences both cost values. For this implementation, the lack of any real-time sensor makes it necessary to use a models to predict the dynamics, in order to calculate the energy cost and thermal comfort. This step executed by using the power and temperature observers.

The observers are needed since, once the chiller setpoint is chosen, there is a resulting evolution on electrical energy consumption as well as on interior temperatures which must be predicted. This is done by maintaining coherence on predicted variables evolution with the chiller setpoint value. The predicted power and temperature variables are determinant on cost calculation in the terms previously described on Chapter 3. The complete of the cost function calculations is presented on Figure 5.1.

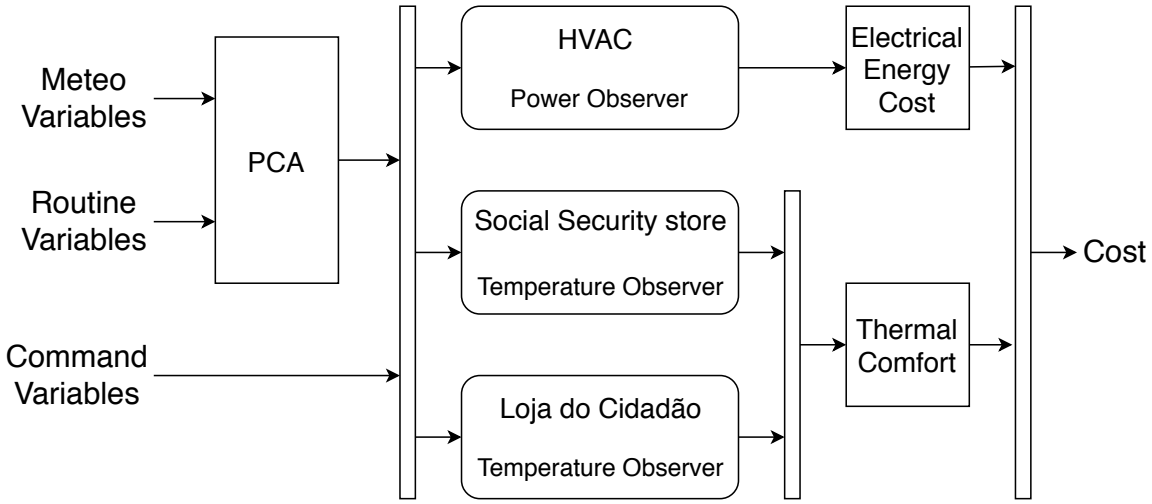

Figure 5.1: Cost function implementation complete diagram

The cost function is divided in three main areas of calculation. The first one for data extraction, done with PCA algorithm, the second one to predict intermediate dynamics, using mathematical models and the third one to calculate the cost, by considering these intermediate values.

The PCA algorithm is applied based on the same vectors calculated during modeling. The data driven modeling of the observers depends upon numerical learning algorithms, a new set of vectors would influence the observer to have different predictions on the same inputs. The calculation of the cost value is based in (3.2) and (3.3), presented on Chapter 3.1 for the predicted values.

5.1.2 Pareto Optimal

On chapter 3.3, it is introduced the Pareto method for dealing with multi-objective optimization. This method consists in finding the points which belong to the Pareto Frontier within the set of results. To have an actual optimization result, there is a need to choose one of these points in order to have a optimal point. There is no unified method to choose the best point, it should be based on the specific case.

The considered method for this dissertation implementation is the *Weighting Method* presented at [20]. It consists in choosing weight values for each objective and giving a certain intuition of the importance of each objective compared with each other. In particular, the weights chosen are 40% for the energy cost and 60% for the thermal comfort one. These weight values are applied on points already obtained and belonging to the Pareto Frontier. The Pareto Optimal is chosen as the point with the smallest cost from the Pareto Frontier, after considering the weighting criteria.

Both objectives scales are in different orders of magnitude. For instance, the energy cost metric is in a unitary order of magnitude and the energy costs in order of magnitude of hundreds to thousands of euros. Before comparing, the values are normalized for the same order of magnitude. On energy cost, there is not a define a bottom bound and for both there is not an upper bound. The normalization scale is, then, defined by the limits on Pareto frontier, which correspond to a scale of 0 to 1.

Chapter 6

Results and Analysis

The system presents an chiller setpoint based on an optimization scenario with a one week duration, starting on a Monday and ending at a Sunday. The optimization is tested on both meta-heuristic algorithms: the PSO and NSGA-III.

The environment conditions tested are one week from one from January of 2018 and one from April of 2018 for heating operating mode and one April of 2017 and one from June of 2018 for the cooling operating mode. To avoid a result presentation overhead, in this chapter is presented one situation for each operating mode on both meta-heuristics. For the heating operating mode, the chosen week starts in 29th January 2018 and ends at 4th February 2018. For the cooling operating mode, the chosen week starts at 25th June 2018 and ends at 1st July 2018.

The graph legends use abbreviated names, to avoid being in front of the graph lines. The ”Org Power” stands for ”Original Power” and ”Opt Power” stands for ”Optimized Power”, corresponding to the acquired power and the power predicted for the optimized setpoint, respectively. The same reasoning is valid for the temperature. The ”Org Temp” is the temperature signal acquired, with the respective setpoint value and ”Opt Temp” is referring to the temperature signal predicted for the optimized setpoint.

6.1 Results of PSO Optimization

The PSO meta-heuristic is configured for the maximum number iteration of 85 with a population size of 10, randomly initialized. On PSO parameters, the inertia weight is 0.5, the personal learning coefficient is 1 and the social learning coefficient is 2. On each scenario, it is presented the graph showing the Pareto solution set, the power and the temperatures, predicted for the optimal setpoint and the real one, in which the data was acquired.

6.1.1 Heating Mode

Figure 6.1 presents a cloud of 10 points, corresponding to the 10 population points. The orange points are the ones belonging to the Pareto frontier, with the green one representing the selected one, following the criteria on chapter **??**. The rest of the points are in blue.

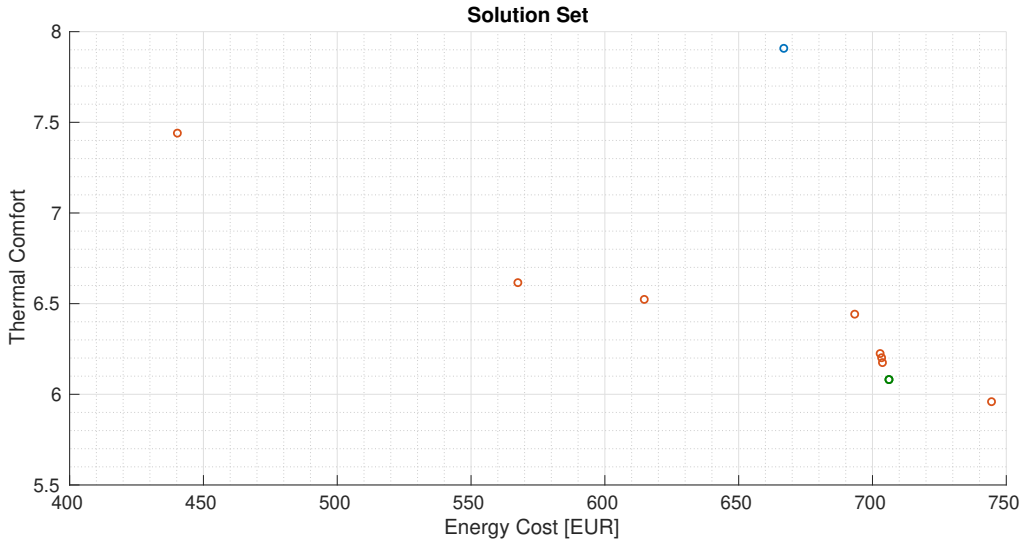

Figure 6.1: Pareto set points for PSO optimization on heating mode from Jan 29 to Feb 05

The chiller setpoints used in Cascais Center were during this week were 42^{o}C in 29th January and 39^{o}C between 31th January and 4th February. The switch happened at 17h of the 30th January. The best point is chosen based at the pareto optimal criteria defined in chapter 5.1.2, which corresponds to a chiller setpoint of 38.23^{o}C. The power used during acquisition real and the predicted one with optimal chiller setpoint is presented in Figure 6.2.

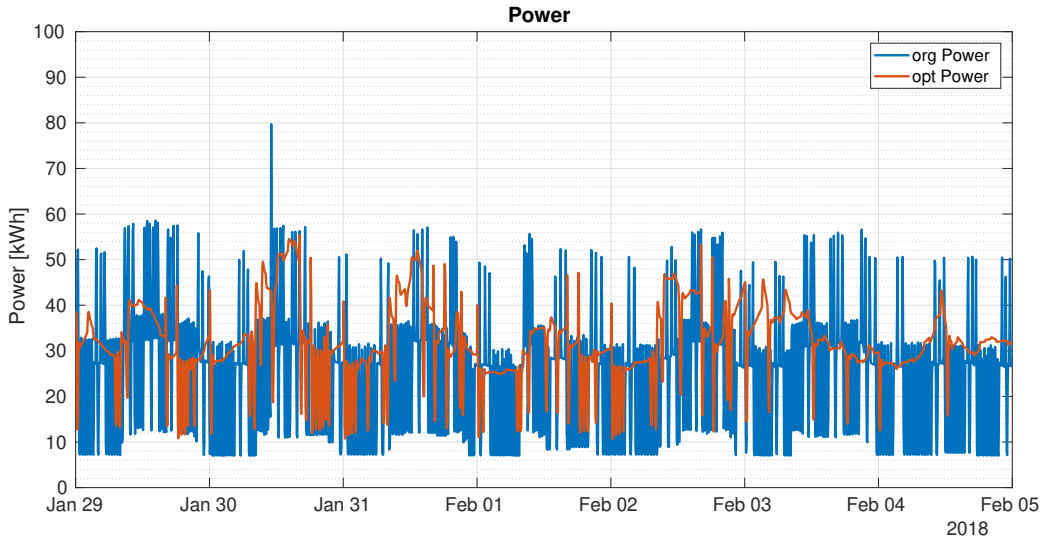

Figure 6.2: HVAC power on acquired and optimized chiller setpoints

From comparing the power evolution from real situation and the prediction one is hard to guess the energy cost value for the optimized chosen chiller setpoint. For this scenario, the optimization results are not satisfactory ones. For this setpoint the energy cost increases from 479.61€ to 614.92€, an increase of 28%. Figure 6.3 presents the real and predicted temperature evolution inside the Social Security store for the already selected chiller setpoint.

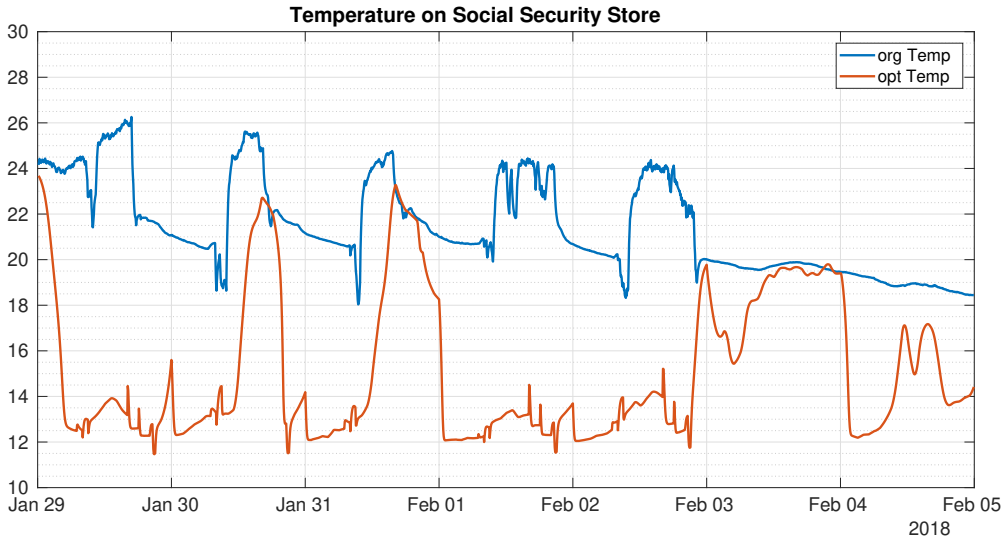

Figure 6.3: Temperature signals on Social Security store for the acquired and the optimized chiller setpoints

The temperature evolution for the optimized chiller setpoint shows a strange predicted dynamic. It shows some rough forms in accordance to an expected behavior of increasing the interior temperature during the day and decreasing during the night. For some parts of the day, the temperature reaches 12^{o}C. This is hardly right, since the temperature was never bellow 15^{o}C on any acquired data. On some parts a difference 0.8^{o}C in chiller setpoint corresponds to a temperature difference of 10^{o}C in interior temperature. These are all evidences of poor modeling. Figure 6.4 presents the real and predicted temperature evolution inside Loja do Cidadão on both chosen thermal zones, for the selected setpoint.

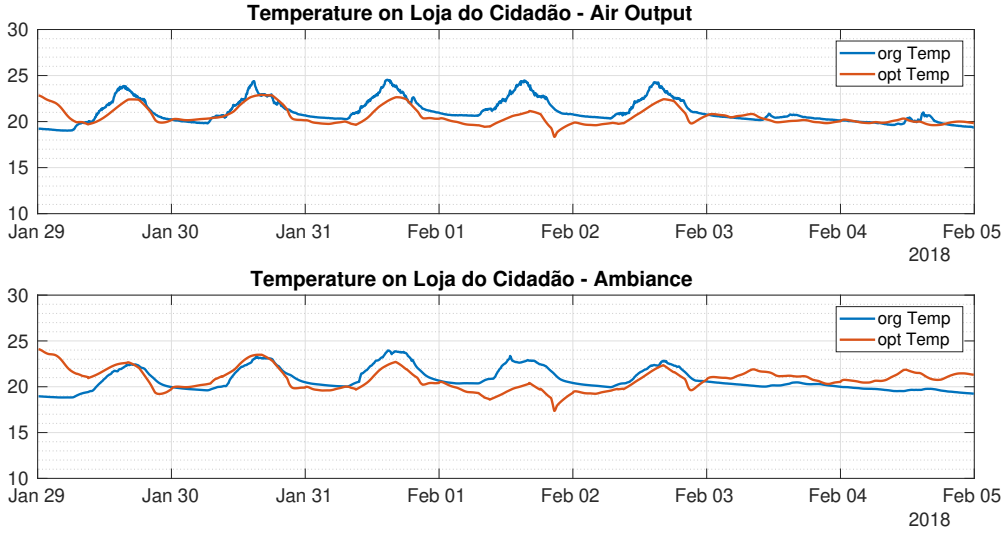

Figure 6.4: Temperature signals on Loja do Cidadão store for the acquired and the optimized chiller setpoints

The temperature evolution in Loja do Cidadão shows a better observer prediction for this store. It is an expected result from the analysis of Section 4.4.2. The observer from Loja do Cidadão showed better performance in all presented situations.

6.1.2 Cooling Mode

Figure 6.5 presents a cloud of 10 points, corresponding to the 10 population points. The color code is the same as before. The orange points are the ones belonging to the Pareto frontier, with the green one representing the selected one, following the criteria on chapter **??**. The rest of the points are in blue.

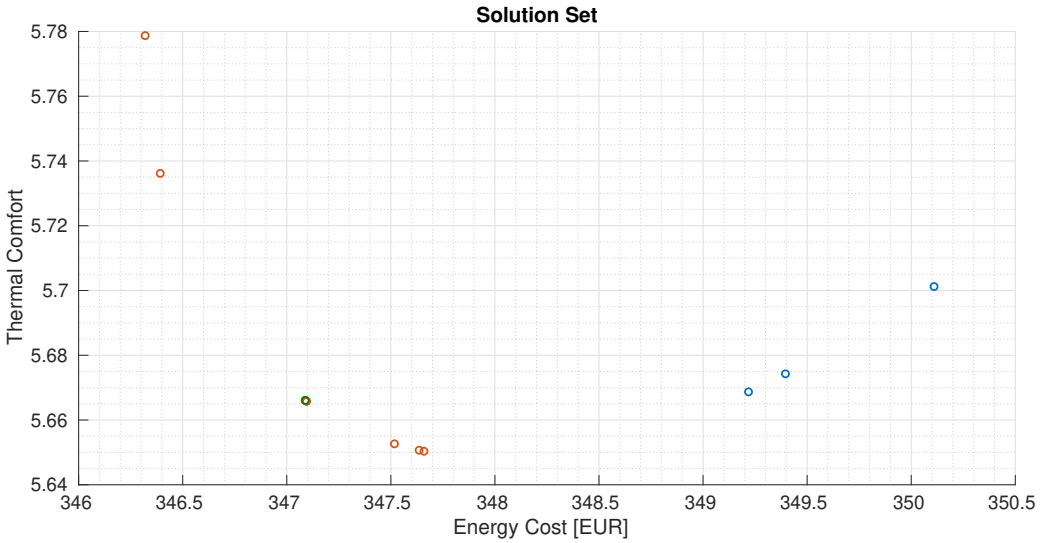

Figure 6.5: Pareto set points for PSO optimization on cooling mode from Jun 25 to Jul 02

The range possible to achieve is a very small one for this cloud of points. The energy cost varies in a range of 4€ and the thermal comfort in a range of 0.14, both are small values on their own scale. The chiller setpoint during this week was 8.5^{o}C. The resulting one from the chosen optimal point is 5.8^{o}C. The Figure 6.6 shows the power signal during acquisition and the predicted one for the optimized setpoint.

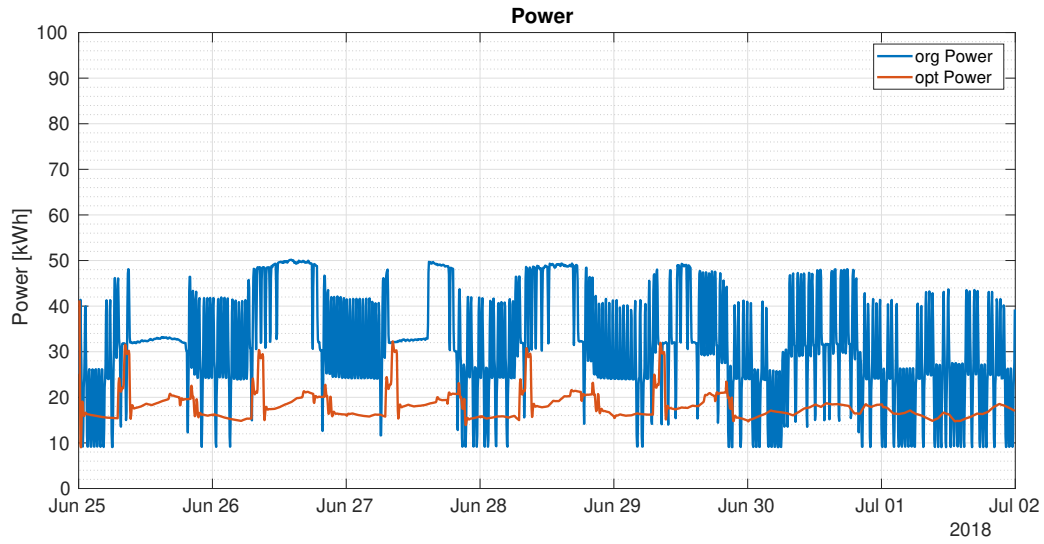

Figure 6.6: HVAC power on acquired and optimized chiller setpoints

In this case, it is noticeable from the graph that on the optimal setpoint there is a considerable

energy consumption spare when compared to the real situation. The energy cost of 626.18 € on the real situation compares with 347.14 € on the optimized setpoint situation, a cost spare of 44.56%. The temperature signals for the acquired and optimized chiller setpoints in Social Security store are presented in Figure 6.7.

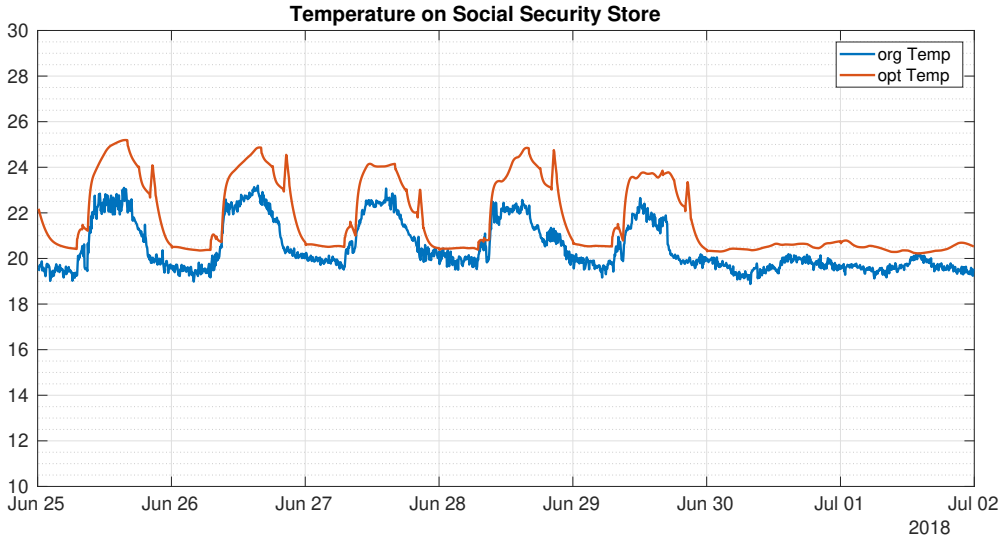

Figure 6.7: Temperature signals on Social Security store for the acquired and the optimized chiller setpoints

The temperature daily evolution shows an average temperature around 23.5^{o}C during a day. Comparing this with the expected comfort temperature observed in Figure 3.1, it is a temperature acceptable for the range of temperatures in Summer. There is an incoherence in results caused by the observer modeling. By comparing the real situation and the one on the optimal setpoint, it seems to exist a smaller effort on the HVAC system for cooling. This result is not an expected one, notice the chiller setpoint on optimized situation is 5.8^{o}C instead of 8.5^{o}C. Figure 6.8 presents the temperatures on Loja do Cidadão for the acquired and optimized setpoints.

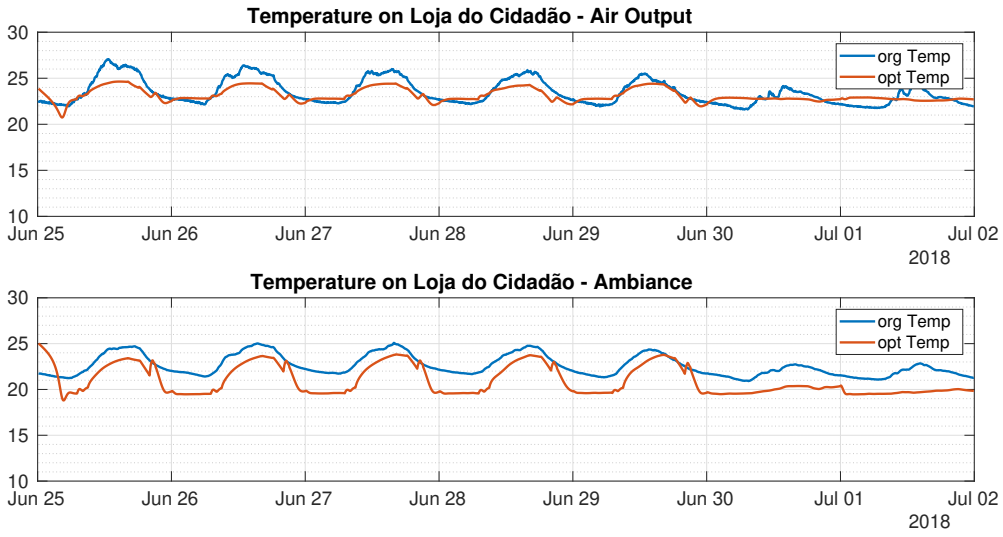

Figure 6.8: Temperature signals on Loja do Cidadão store for the acquired and the optimized chiller setpoints

The temperature evolution inside Loja do Cidadão is a more coherent one for the selected chiller setpoint. While it shows a higher cooling effort by having a lower temperature in almost all samples during the day, it keeps the average temperature in near the 23^{o}C.

6.2 Results of NSGA-III Optimization

For the NSGA-III meta-heuristic, there are presented the same situations as in PSO, one for each operating mode. The maximum iteration number is 50 with a population size of 10, randomly initialized. The NSGA-III is configured with crossover ratio of 0.5 and a mutation rate of 0.02. On each scenario, it is presented the graph showing the Pareto solution set, the power and the temperatures, predicted for the optimal setpoint and the real one, in which the data was acquired.

6.2.1 Heating Mode

The Figure 6.9 presents a cloud of 10 points, corresponding to the 10 population points. The orange points are the ones belonging to the Pareto frontier, with the green one representing the selected one, following the criteria on chapter **??**. The rest of the points are in blue.

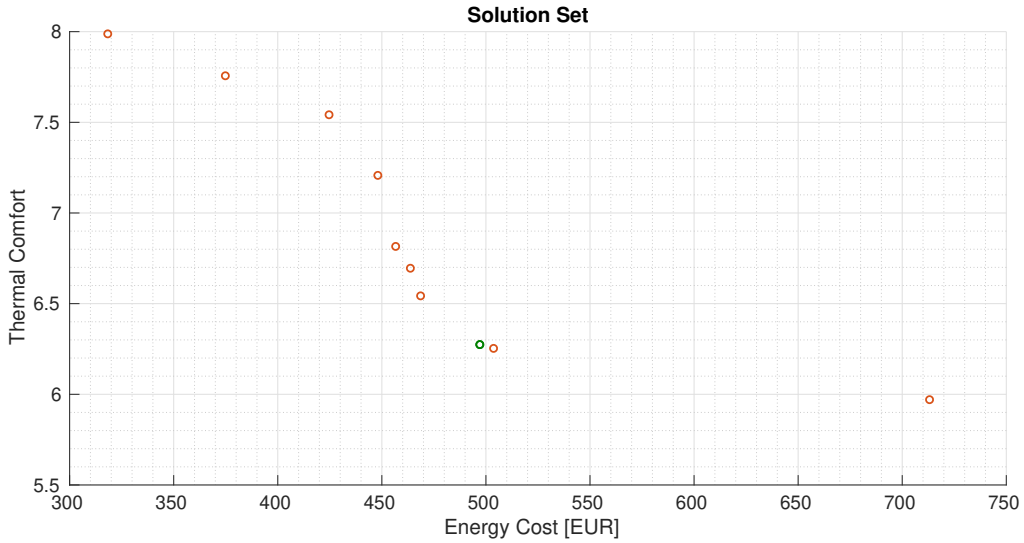

Figure 6.9: Pareto set points for NSGA-III optimization on heating mode from Jan 29 to Feb 05

In the presented case, all population points converged into points present in the Pareto frontier. The setpoints are the same as before: 42^{o}C in 29th January and 39^{o}C between 31th January and 4th February. The switch happened at 17h of the 30th January. The optimal setpoint is 39^{o}C. The power used during acquisition real and the predicted one with optimal chiller setpoint is presented in Figure 6.10.

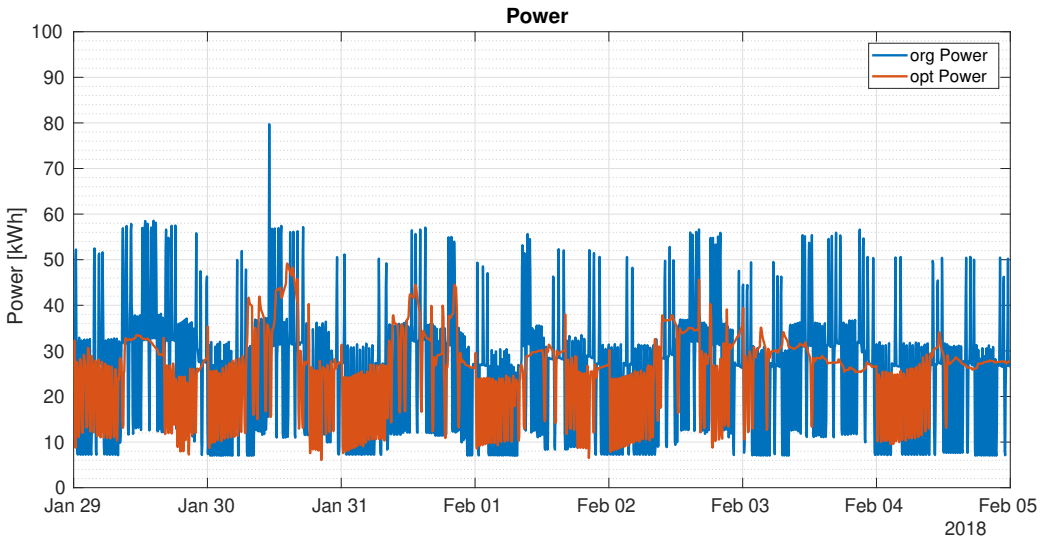

Figure 6.10: HVAC power on acquired and optimized chiller setpoints

The real and optimal chiller setpoints produce similiar energy costs. The real situation costed 379.61 €. The optimized setpoint situation have a cost of 397.29 €, an increase of 3.68% in energy cost. The energy costs in the real situation and the optimized one are closer in this case. The reason is clear, a significant part of the week, the setpoint is the same for both situations. The Figure 6.11 shows the temperature inside the Social Security store during the same period.

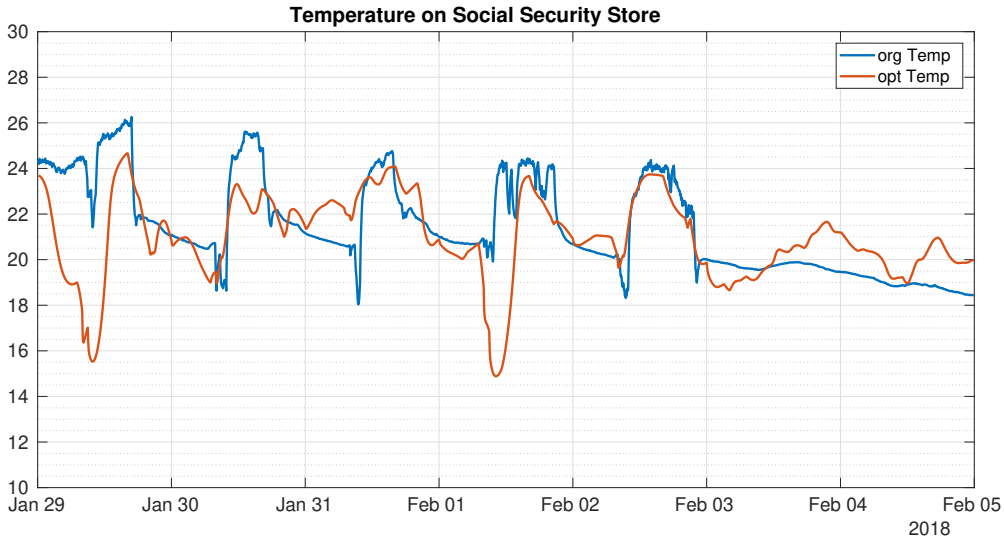

Figure 6.11: Temperature signals on Social Security store for the acquired and the optimized chiller setpoints

The temperature inside Social Security store presented on Figure 6.11 shows a much more coherent dynamic than the previous situations presented. The duration in which the setpoint is coincident for both situations, there is not an high error in between both temperatures in terms of values (there is a dynamic difference, though). For the temperature in first days presented, there is a big decreasing around the opening of the store. This is a modeling flaw in the observer, which considers the effort on the optimized not to be enough to increase the temperature on the store opening. This is the time of the day where the most effort is required since there is too little actuation from the HVAC during night. The resulting predicting dynamic is not an expected one to happen. In Figure 6.12, it is presented the temperature inside Loja do Cidadão during the same period.

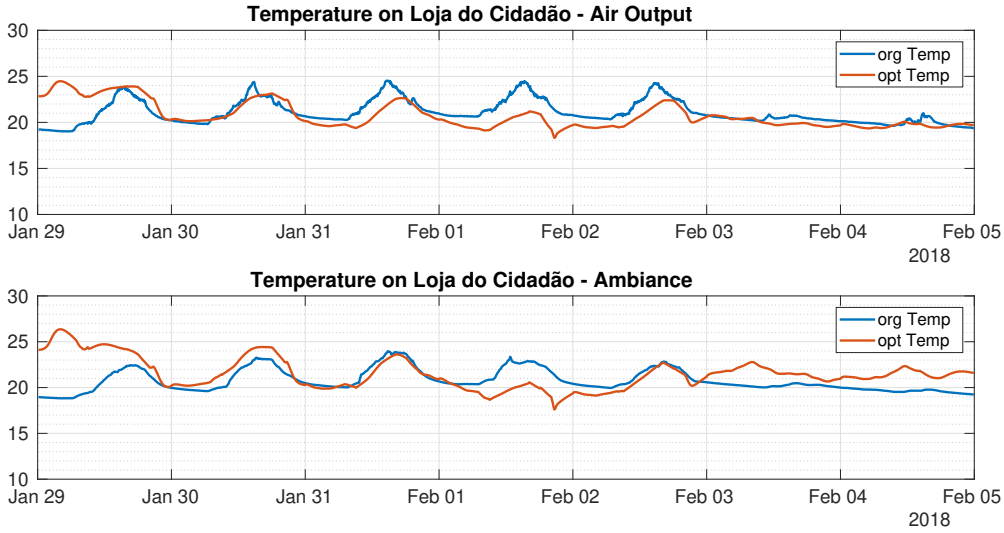

Figure 6.12: Temperature signals on Loja do Cidadão store for the acquired and the optimized chiller setpoints

The temperature in Loja do Cidadão showed an evolution very similar to the one presented in PSO

optimization. The modeling shows smaller changes to a change on setpoint than for the Social Security store.

6.2.2 Cooling Mode

The Figure 6.13 presents a cloud of 10 points, corresponding to the 10 population points. The color code is the same as before. The orange points are the ones belonging to the Pareto frontier, with the green one representing the selected one, following the criteria on chapter **??**. The rest of the points are in blue.

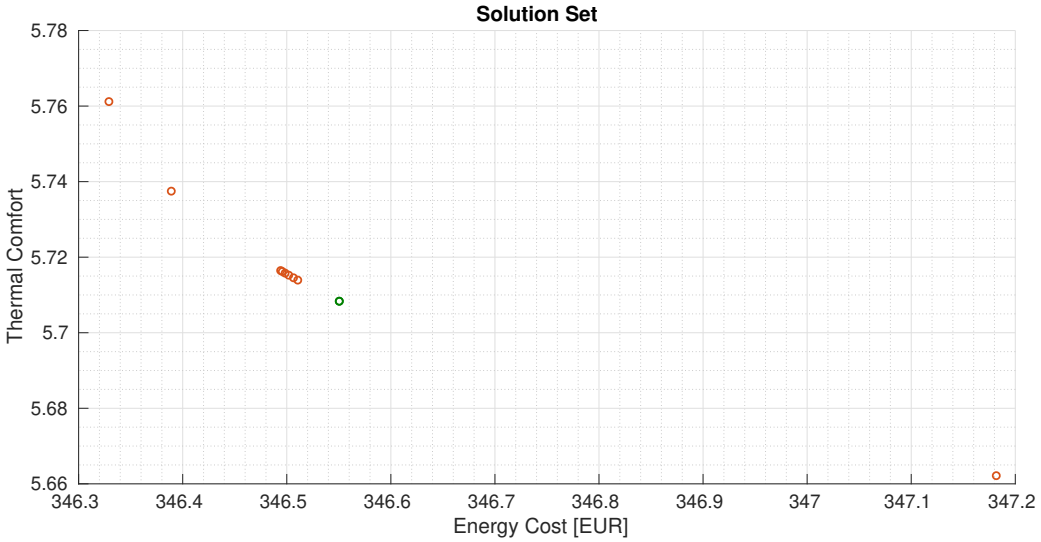

Figure 6.13: Pareto set points for NSGA-III optimization on cooling mode from Jun 25 to Jul 02

The same happened as the last optimization scenario on NSGA-III algorithm, the entire population converged to the Pareto frontier. The population is in the same interval as in PSO result. During the entire duration the setpoint was 8.5^{o}C in real situation. The setpoint which corresponds to the chosen point is 6.0^{o}C. The Figure 6.14 presents the power in the same scenario.

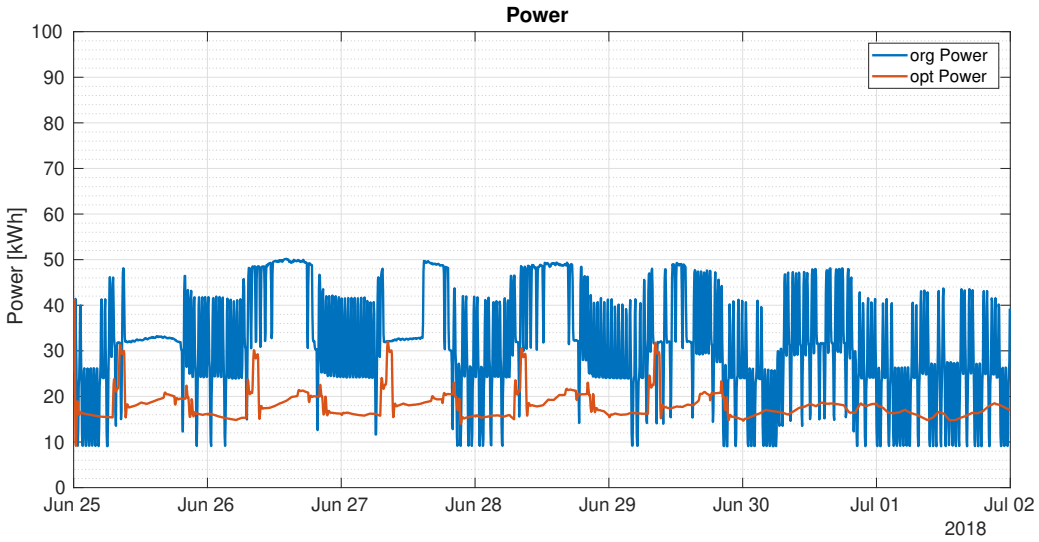

Figure 6.14: HVAC power on acquired and optimized chiller setpoints

The power usage is almost the same as in the same scenario on the PSO optimization. The result is expected, the setpoint is almost the same as before. The cost of 626.18 € on the real situation compares with a cost of 346.60 € in the optimized setpoint, a spare of 44.65%. The temperature inside Social Security store is presented in Figure 6.15.

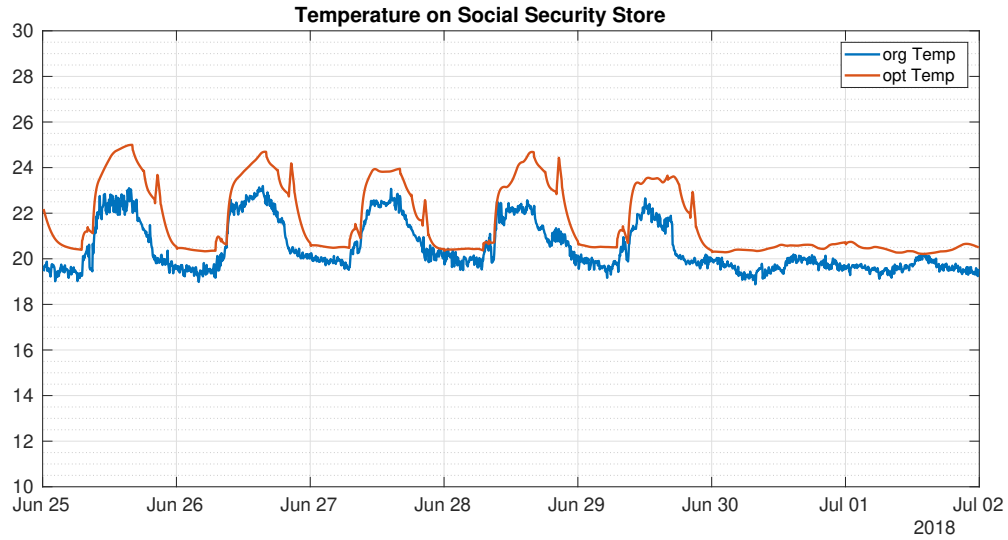

Figure 6.15: Temperature signals on Social Security store for the acquired and the optimized chiller setpoints

The temperature inside Social Security store shows almost the same dynamic as in PSO optimized case, as it would be expected. Figure 6.16 presents the temperature signals on Loja do Cidadão.

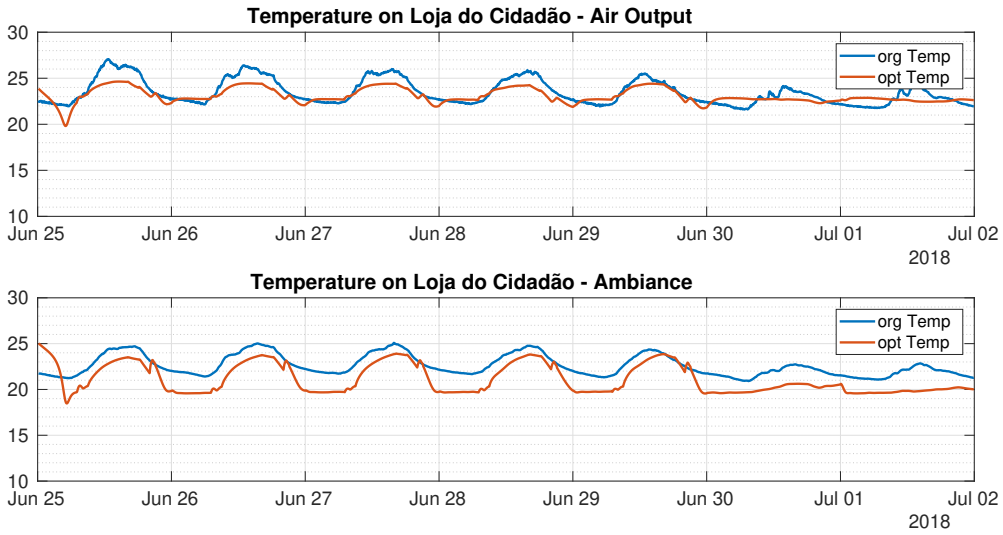

Figure 6.16: Temperature signals on Loja do Cidadão store for the acquired and the optimized chiller setpoints

The temperature inside Loja do Cidadão shows the same dynamics ad the one presented on the PSO optimization.

Chapter 7

Conclusions

Previous chapters showed the followed steps to complete this dissertation in a way it can be applicable to another project. Other projects may use the same concepts as this one, with the natural adaptations on the characteristics of their case study. The Cascais Center as a case study had an important role during dissertation in defining the set of procedures to be taken.

In this chapter, there is a brief overview on how the methodology applied applied worked, how it would be better and also point out major concerns to have when applying it. Next, the priority tasks are described in order to continue improving the method and its performance.

7.1 Achievements

This master thesis presents a method to improve the HVAC system usage based on open-loop optimal control applied on the chiller setpoint. This dissertation allowed to construct a start to end method of an external system to apply optimal control to a generic HVAC system.

The results obtained on the Cascais Center implementation are, however, not conclusive on the complete success of the methodology used. The reason is that, for an optimal optimization method to work, there is a need of a ”good” model. In this dissertation, the observers served this objective. Their performance revealed, however, not a good enough one for the control strategy to result. During the data acquisition, there were constraints in logger devices availability and also in schedule availability to acquire data on Cascais Center. This is a critical issue, considering the project uses data-driven modeling. Having a poor model sensitivity to the variable to optimize is a major bottleneck during the optimization process.

The observer modeling allowed the comparison on two different methods. The NARX Neural Network predictive model showed much better results when compared to Takagi-Sugeno method, following the literature available for predictive control on HVAC systems, which give an higher emphasis on this type of model. Despite that, it is worth to notice both models are not equally implemented. The NARX Neural Network used is a well known implementation on a consecrated mathematical software. The Takagi-Sugeno implementation used is one implementation developed during this dissertation, with

a more limited number of features available and less parameters possible to change in order to fine tune results. On chapter 7.2, there is a suggestion on an improved implementation on Takagi-Sugeno method which may improve results on this type of project.

On the optimization side, both meta-heuristics achieved expected results. The main difference between both is more of a convergence one. The NSGA-III converges in a smaller number of iterations than PSO. The optimization is still possible to improve, though. In chapter 7.2, there are two suggested methods to improve the adaptive thermal comfort and user input configuration.

There is an important consideration to be made on the optimization scenario. It is not realistic to have a short duration on a setpoint which is only manually changed. Despite that, the prediction methods improve their results as the predicted sample gets closer. In an implementation, the prediction is part of the system, but also of the data, since the meteorological data is also predicted.

7.2 Future Work

Despite the results obtained during this dissertation, there is room for improvement. For this metodology to present good results, it is critical to change the general scope arround which the work is developed. There is a need for a more access on new data acquirement and scenario testing in real device. This Section aims to present the steps identified to be the natural ones to improve in future, considering the results obtained during this disseration. Each improvement is described in separate way, though, none of them is incompatible with the others.

Decoupling Data Acquirement on HVAC Modules

The complete HVAC system has a highly complex and non-linear dynamic. Each part of the system reacts differently to user inputs as well as the environment variables. Having the data acquired separately in modules or partially decoupled can improve the usage of the data during the modeling process. The individual dynamic on each part of the HVAC (chiller, air handler, fans) is an easier one to observe than the total one. A good observer would depend on a good integration on the observers of each module. The modeling may become a more robust one for data not available on dataset. For instance, a contained user input variable of another module does not have the same influence on the first one.

Adaptive Thermal Comfort

The thermal comfort, as described in [13], depends on lots of factors. Most of them are very hard to measure and highly variable. Some even depend on room characteristics. For instance, the thermal comfort models could be different ones either for National Insurance store or Loja do Cidadão. The thermal comfort can be estimated by used a supervised learning model [12]. It may include indirectly features related to the room itself, for example, a more rigorous temperature expectation estimation. A supervised learning model may even include value variation into the thermal comfort estimation. Notice

that it is a subjective metric of an human sensation. A model of this kind needs a participation of many people during a relatively long duration to have statistical significance.

Takagi-Sugeno Differential Implementation

On every observer, the NARX Neural Network model showed much better performance than the Takagi-Sugeno. The NARX Neural Network model relies on previous outputs feedback, with are usually important information in prediction for dynamic systems. The Takagi-Sugeno model is frequently used without feedback. Though, the Takagi-Sugeno predicting performance may be improved by predicting variations instead of the real value [9]. In this implementation, the observe will not predict the output real value, but a difference to the last sampling period output.

Occupancy Estimation

The occupancy is one of the most influent parameters on interior temperatures and energy consumption dynamics. An higher occupancy effects in an interior temperature increase. While on heating operating mode, this impacts on a energy consumption decrease but on cooling mode, it is the opposite. In either case, for both stores, considering the amount of people inside, its effect is not negligible.

During the modelling process, the rotine variables showed an high influence in observed variables dynamics, following the results of [8]. It is a parameter for the dynamic and can be used as a input for the other observers. The best-suited implementation is to use a data-driven supervised for temperature estimator. However, if this data is not available, it can be indirectly estimated (for instance, using the air humidity concentration) or using a rough estimation by intervals, based on local observation. Both these alternatives may improve the results obtained by different degrees.

Command Input Optimization

On complex non-linear systems, the changing of one parameter have an non-linear influence on others, either positive or negative. A multi-objective optimization method applied on a major number of freedom degrees tend to achieve better results than an application for each part. The difference in approach is to find an optimized set of inputs instead on individually optimized inputs. The set of inputs may included, for instance, the temperature setpoints of both chillers, heating and cooling pumps ON/OFF command, the air handlers temperature setpoint and ON/OFF schedules.

The optimization complexity increases by optimizing a higher number of parameters. The objective function and the points from Pareto set have an higher dimension. The observers depend upon a higher number of inputs, increasing the models complexity. The consequence is to have a slower and to have an higher computational cost. The optimized variables vary in real and binary types and the period in which the value changes is different on each of them. In each scenario, there is a set of values per sample for each variable, from which the cost values are obtained.

Bibliography

[1] A. energy regulatory. Hvac hess factsheets. URL https://www.energy.gov.au/sites/g/files/net3411/f/hvac-factsheet-basics-energy-efficiency.pdf.

[2] enerdata. Electrical energy comsumption. URL https://yearbook.enerdata.net/electricity/electricity-domestic-consumption-data.html.

[3] U. of Michigan. Build environment factsheets. URL http://css.umich.edu/sites/default/files/Residential_Buildings_Factsheet_CSS01-08_e2017.pdf.

[4] M. A. Lopes. Optimizing Energy Consumption in the Civil Engineering Building. Master's thesis, Instituto Superior Técnico, 2017.

[5] H. Pombeiro. *Intelligent energy management in buildings: unfolding a new set of approaches centered in the users*. PhD thesis, Instituto Superior Técnico, 2016.

[6] F. Tang. HVAC system modeling and optimization: a datamining approach. Master's thesis, University of Iowa, 2010.

[7] Y. Kim. Optimal Price-Based Demand Response of HVAC Systems in Multi-Zone Office Buildings Considering Thermal Preferences of Individual Occupants. *IEEE Transactions on Industrial Informatics*, 2018.

[8] Z. Wang, Y. Wang, and R. S. Srinivasan. A novel ensemble learning approach to support building energy use prediction. *Energy and Buildings*, 2018.

[9] J. Teeter and M. Y. Chow. Application of functional link neural network to hvac thermal dynamic system identification. *IEEE Transactions on Industrial Electronics*, 1998.

[10] S. Li, S. Ren, and X. Wang. HVAC Room Temperature Prediction Control Based on Neural Network Model. *Measuring Technology and Mechatronics Automation (ICMTMA), 2013 Fifth International Conference on*, 2013.

[11] H. Huang, L. Chen, and E. Hu. A neural network-based multi-zone modelling approach for predictive control system design in commercial buildings. *Energy and Buildings*.

[12] P. M. Ferreira, S. M. Silva, A. E. Ruano, A. T. Négrier, and E. Z. Conceição. Neural network PMV estimation for model-based predictive control of HVAC systems. *Proceedings of the International Joint Conference on Neural Networks*, 2012.

[13] ANSI/ASHRAE 55-2010. *ANSI/ASHRAE 55 Thermal Environmental Conditions for Human Occupancy*, 2010.

[14] URL https://www.cascais.pt/sites/default/files/styles/galeria-new/public/imagens/noticias/loja_cidadao_cascais_01.png?itok=jZ1Oz-TP.

[15] R. McDowall. *Fundamentals of HVAC Systems: SI Edition*. Elsevier, 1^{st} edition, 2007. ISBN: 978-0-12-373998-8.

[16] URL http://www.astena.ru/PRIBORS/fluke-1735.jpg.

[17] URL https://s3.eu-west-1.amazonaws.com/gemini2.assets.d3r.com/images/product_detail/6587-tk-4014-talk-2-data-logger.jpg.

[18] yarpiz. URL http://yarpiz.com/category/metaheuristics.

[19] M. D. Somma. URL https://www.researchgate.net/profile/Marialaura_Di_Somma/publication/309609991/figure/fig6/AS:423898740203527@1478076743783/Example-of-a-Pareto-frontier-for-a-multi-objective-optimization-problem-with-two.png.

[20] J. Branke, K. Deb, K. Miettinen, and R. Slowinski. *Multiobjective Optimization: Interactive and Evolutionary Approaches*. 2008. ISBN 978-3-540-88907-6.

[21] K. L. Du and M. N. Swamy. *Search and optimization by metaheuristics: Techniques and algorithms inspired by nature*. 2016. ISBN 978-3-319-41191-0.

[22] I. T. Jolliffe. *Principal Component Analysis*. Encyclopedia of Statistics in Behavioral Science, 2^{nd} edition, 2002. ISBN: 978-0-387-22440-4.

[23] D. Ruan. *Intelligent Hybrid Systems: Fuzzy Logic, Neural Networks, and Genetic Algorithms*. Springer Science+Business Media, LLC, 1^{st} edition, 1997. ISBN: 978-1-4613-7838-9.

[24] E. Poço. Optimizing the Energy Efficiency of Commercial Buildings. Master's thesis, Instituto Superior Técnico, 2015.

[25] I. Montes. Intelligent Estimation of LiFePO4 Battery State-of-Charge (SOC) in Electric Vehicles. Master's thesis, Instituto Superior Técnico, 2016.

[26] P. Branco. *Aprendizagem por exemplos utilizando lógica "fuzzy" na modelização e controlo de um accionamento electro-hidráulico*. PhD thesis, Instituto Superior Técnico, 1998.

[27] H. T. Siegelmann, B. G. Horne, and C. L. Giles. Computational capabilities of recurrent NARX neural networks. *IEEE Transactions on Systems, Man, and Cybernetics, Part B: Cybernetics*, 1997.

[28] A. Kusiak and G. Xu. Modeling and optimization of HVAC systems using a dynamic neural network. *Energy*, 2012.

[29] E. B. Solovyeva. Types of Recurrent Neural Networks For Non-linear Dynamic System Modelling. 2017.

[30] Z. Afroz, G. M. Shafiullah, T. Urmee, and G. Higgins. Modeling techniques used in building HVAC control systems: A review. *Renewable and Sustainable Energy Reviews*, 2017.

[31] R. Zemouri, R. Gouriveau, and N. Zerhouni. Defining and applying prediction performance metrics on a recurrent NARX time series model. 2010.

[32] M. Aafaque and M. B. Kadrit. Dynamic Fuzzy Modelling of Cooling Coil System. 2014.

[33] L. B. de Almeida. *Multilayer Perceptrons*.

[34] L. B. de Almeida. *An introduction to principal components analysis*, 2015.

[35] J. Blondin. *Particle swarm optimization: A tutorial*, 2009.

[36] meteoblue. URL `https://www.meteoblue.com`.

[37] Relatório de Climatização e Ventilação no Cascais Center. Technical report.

Appendix A

Data Statistics

On chapter 2.5, it were presented preliminary results based on a broad analysis to acquired data. This appendix presents it in a a more detailed way. These results are presented to give the reader a better intuition on the data in terms of distribution and orders of magnitude and support the analysis carried out over the dissertation.

The statistic results are presented separately for each acquirement period. The abbreviations have the same meaning as in chapter 2.5. The interior temperature is measured in Social Security Store (SSS), Loja do Cidadão - Air Out (LCO) and Loja do Cidadão - Ambiance (LCA). The thermal comfort is calculated for each store, the Social Security Store (SSS) and the Loja do Cidadão (LC).

Table A.1: Preliminary results on data of April of 2017

April 2017								
Date	**Energy [kWh]**	**Energy Cost [€]**	**Av. Temp. Outside [^{o}C]**	**Av. Temp. Inside [^{o}C]**			**Thermal Comfort**	
				SSS	**LCO**	**LCA**	**SSS**	**LC**
08/04/2017	511.61	61.20	16.52	21.92	23.29	22.74	0.00	0.00
09/04/2017	359.71	41.73	16.23	21.75	23.51	22.78	0.00	0.00
10/04/2017	563.85	68.31	19.22	22.62	23.44	23.26	3.31	3.41
11/04/2017	571.40	69.16	17.35	23.35	24.24	24.08	2.24	2.47
12/04/2017	549.09	66.83	16.93	21.94	23.85	23.73	2.36	2.42
13/04/2017	544.68	66.25	16.11	20.86	22.67	22.79	2.93	3.04
14/04/2017	510.15	61.79	16.10	19.96	22.36	22.09	3.02	3.06
15/04/2017	518.70	62.42	15.33	19.64	22.13	21.66	0.00	0.00
16/04/2017	369.53	43.25	16.34	20.93	22.87	22.10	0.00	0.00

Table A.2: Preliminary results on data of September of 2017

September 2017								
Date	Energy [kWh]	Energy Cost [€]	Av. Temp. Outside [^{o}C]	Av. Temp. Inside [^{o}C]			Thermal Comfort	
				SSS	LCO	LCA	SSS	LC
12/09/2017	900.89	107.30	19.71	19.78	23.88	22.58	1.92	2.30
13/09/2017	984.95	118.07	19.68	20.46	23.75	21.96	2.04	2.48
14/09/2017	848.58	099.63	18.78	20.31	23.49	21.82	3.00	3.12
15/09/2017	734.56	086.04	17.73	19.05	22.66	20.79	3.00	3.00
16/09/2017	650.33	075.76	17.18	17.98	21.61	19.62	0.00	0.00
17/09/2017	612.90	070.61	17.81	17.78	21.24	19.30	0.00	0.00
18/09/2017	717.28	084.61	18.90	18.60	21.93	20.46	3.01	3.01

Table A.3: Preliminary results on data of January of 2018

January 2018								
Date	Energy [kWh]	Energy Cost [€]	Av. Temp. Outside [^{o}C]	Av. Temp. Inside [^{o}C]			Thermal Comfort	
				SSS	LCO	LCA	SSS	LC
23/01/2018	621.18	244.79	13.02	20.54	21.41	21.08	3.00	3.00
24/01/2018	640.11	265.85	10.99	21.33	21.08	20.78	3.00	3.00
25/01/2018	671.32	250.86	12.20	21.17	20.99	20.78	3.00	3.00
26/01/2018	693.87	253.14	10.71	22.46	20.85	20.56	3.00	3.00
27/01/2018	741.06	292.46	10.67	24.05	19.78	19.32	0.00	0.00
28/01/2018	576.78	272.75	11.03	24.16	19.50	18.98	0.00	0.00
29/01/2018	682.23	270.94	12.76	23.70	20.82	20.33	3.20	3.22
30/01/2018	584.52	225.62	13.01	22.07	21.29	21.08	3.04	3.10
31/01/2018	550.59	216.08	12.57	21.87	21.69	21.57	3.20	3.22
01/02/2018	546.64	236.06	10.52	22.11	21.79	21.41	3.00	3.00
02/02/2018	616.87	234.19	09.25	21.63	21.62	21.05	3.00	3.00
03/02/2018	629.56	256.82	10.14	19.74	20.43	20.25	0.00	0.00
04/02/2018	500.88	222.03	08.99	18.93	19.91	19.64	0.00	0.00
05/02/2018	625.04	237.19	09.38	19.71	20.31	19.95	3.00	3.00

Table A.4: Preliminary results on data of April of 2018

April 2018								
Date	Energy [kWh]	Energy Cost [€]	Av. Temp. Outside [^{o}C]	Av. Temp. Inside [^{o}C]			Thermal Comfort	
				SSS	LCO	LCA	SSS	LC
27/03/2018	461.88	52.62	12.72	22.31	23.59	21.97	3.00	3.00
28/03/2018	499.10	56.93	10.76	21.99	24.91	23.38	3.00	3.00
29/03/2018	478.27	55.64	10.60	22.34	25.00	23.72	3.00	3.00
30/03/2018	531.94	61.60	10.70	21.74	24.80	23.39	3.00	3.00
31/03/2018	475.36	54.87	12.19	21.58	24.91	23.40	0.00	0.00
01/04/2018	532.74	62.89	13.17	21.50	24.73	23.29	0.00	0.00
02/04/2018	397.35	45.03	13.44	22.56	24.74	23.79	3.00	3.00
03/04/2018	366.92	42.65	14.04	23.07	24.27	23.32	3.00	3.00
04/04/2018	410.18	47.51	13.60	23.44	24.42	23.14	3.00	3.00
05/04/2018	440.90	50.35	12.27	23.24	23.82	22.63	3.00	3.00
06/04/2018	416.23	48.35	12.74	22.26	22.34	22.14	3.00	3.00
07/04/2018	488.64	56.94	11.91	21.45	21.58	20.71	0.00	0.00
08/04/2018	357.58	38.66	10.99	20.55	20.77	19.81	0.00	0.00

Table A.5: Preliminary results on data of June of 2018

June 2018								
Date	**Energy [kWh]**	**Energy Cost [€]**	**Av. Temp. Outside [^{o}C]**	**Av. Temp. Inside [^{o}C]**			**Thermal Comfort**	
				SSS	**LCO**	**LCA**	**SSS**	**LC**
19/06/2018	919.74	108.3	22.32	21.11	23.89	23.45	1.30	1.80
20/06/2018	1164.6	143.3	24.01	21.99	24.23	23.58	3.29	3.12
21/06/2018	927.35	110.0	22.37	21.77	24.06	23.63	2.64	2.73
22/06/2018	1086.2	132.7	23.02	22.10	24.90	24.30	2.68	2.50
23/06/2018	786.20	90.17	20.96	20.52	24.23	23.27	0.00	0.00
24/06/2018	695.86	80.40	19.37	20.07	23.60	22.48	0.00	0.00
25/06/2018	703.02	82.45	17.24	20.70	24.10	22.85	3.00	3.01
26/06/2018	926.42	109.4	17.33	20.92	24.05	23.09	3.04	3.11
27/06/2018	813.84	93.61	17.71	20.94	23.84	23.08	3.04	3.06
28/06/2018	877.43	103.9	18.19	20.91	23.71	22.98	3.05	3.11
29/06/2018	764.99	89.28	17.64	20.50	23.38	22.62	3.14	3.14
30/06/2018	695.42	82.11	17.55	19.67	22.63	21.74	0.00	0.00
01/07/2018	567.61	65.80	17.89	19.63	22.64	21.74	0.00	0.00
02/07/2018	740.20	87.13	17.80	20.28	23.36	22.32	3.00	3.00

Appendix B

Dataset Partition

On chapter 4.3 it is described the main criteria used to make the partitions on data in order to used in different supervised learning models. The Tables B.1 and B.2 present the resulting division on the real acquired data for heating and cooling cases, respectively, based on those criteria. The sets are represented by the same color scheme as in chapter 4.3. The training set is represented in blue, the validation set in green and the test set in red.

For the heating operating mode, there are data from 27 days available on dataset, with 15 selected for training set, 6 for validation set and 6 for test set.

Table B.1: Dataset partition for heating operating mode

January 2018			April 2018		
Date	**Week Day**	**Set**	**Date**	**Week Day**	**Set**
23/01/2018	Tuesday		27/03/2018	Tuesday	
24/01/2018	Wednesday		28/03/2018	Wednesday	
25/01/2018	Thursday		29/03/2018	Thursday	
26/01/2018	Friday		30/03/2018	Friday	
27/01/2018	Saturday		31/03/2018	Saturday	
28/01/2018	Sunday		01/04/2018	Sunday	
29/01/2018	Monday		02/04/2018	Monday	
30/01/2018	Tuesday		03/04/2018	Tuesday	
31/01/2018	Wednesday		04/04/2018	Wednesday	
01/02/2018	Thursday		05/04/2018	Thursday	
02/02/2018	Friday		06/04/2018	Friday	
03/02/2018	Saturday		07/04/2018	Saturday	
04/02/2018	Sunday		08/04/2018	Sunday	
05/02/2018	Monday		-	-	-

For the cooling operating mode, there are data from 30 days available on dataset, with 20 selected for training set, 5 for validation set and 5 for test set.

Table B.2: Dataset partition for cooling operating mode

April 2017			September 2017			June 2018		
Date	**Week Day**	**Set**	**Date**	**Week Day**	**Set**	**Date**	**Week Day**	**Set**
08/04/2017	Saturday		12/09/2017	Tuesday		19/06/2018	Tuesday	
09/04/2017	Sunday		13/09/2017	Wednesday		20/06/2018	Wednesday	
10/04/2017	Monday		14/09/2017	Thursday		21/06/2018	Thursday	
11/04/2017	Tuesday		15/09/2017	Friday		22/06/2018	Friday	
12/04/2017	Wednesday		16/09/2017	Saturday		23/06/2018	Saturday	
13/04/2017	Thursday		17/09/2017	Sunday		24/06/2018	Sunday	
14/04/2017	Friday		18/09/2017	Monday		25/06/2018	Monday	
15/04/2017	Saturday		-	-	-	26/06/2018	Tuesday	
16/04/2017	Sunday		-	-	-	27/06/2018	Wednesday	
-	-	-	-	-	-	28/06/2018	Thursday	
-	-	-	-	-	-	29/06/2018	Friday	
-	-	-	-	-	-	30/06/2018	Saturday	
-	-	-	-	-	-	01/07/2018	Sunday	
-	-	-	-	-	-	02/07/2018	Monday	